MINISTRY OF HIGHER EDUCATION AND SCIENTIFIC RESEARCH

TRAINING AND RESEARCH UNIT
SCIENCES OF STRUCTURES OF MATTER AND TECHNOLOGY

REPUBLIC OF CÔTE D'IVOIRE

UNION - DISCIPLINE - WORK

Felix houphouet-boigny university

INSTITUTE OF BIO-AND GEOSCIENCES-AGROSPHERE

Nº: 667

MASTER IN RENEWABLE ENERGY AND CLIMATE CHANGE

SPECIALITY: GREEN HYDROGEN/GEORESOURCES

MASTER THESIS:

Subject/TOPIC:

Impact of changing climate on the potential of streamflow for hydropower generation in Africa, Genale Dawa III(GD-3) in Ethiopia

Presented Date 08/,2023 by:

JALLAH JOE BLAMA

JURY:

Prof. KOUADIO Yves	**President**	**Senior Lecturer at UFHB**
Dr (MC) TOUALY Elisée	**Examiner**	**Senior Lecturer at UFHB**
Dr (MC) FASSINOU Wanignon Ferdinand	**Main Supervisor**	**Senior Lecturer at UFHB**
Prof. Harrie-Jan Hendricks-Franssen	**Co-Supervisor**	**Head of research at (IBG-3) Forschungszentrum Jülich GmbH**

Academic year: 2022-2023

CANDIDATE'S DECLARATION

I hereby declare that this Master's thesis is the result of my research, and that no part of it has been presented for another degree at this university or elsewhere.

Name: _____

Candidate's signature:_____Date: _____

ACKNOWLEDGEMENT

I would like to express my heartfelt gratitude to the West Africa Science Center on Climate Change and Adapted Land Use (WASCAL) and Bundesministerium für Bildung und ForschungBMBF (Federal Ministry of Education and Research) for their support throughout my studies. I am immensely grateful to the president of the University of Abou Moumouni Niger and the President of the University of Felix Houphouet-Boigny of Cote d'Ivoire for their guidance and encouragement. I would also like to extend my thanks to the Director of the Institute of Georesources and Materials Engineering, Faculty Agrosphere (IBG3), Forschungszentrum Julich, Germany, for their valuable assistance during my research. Additionally, my appreciation goes to the directors and deputy directors of the respective universities, Prof. Rabani Adamou, and Dr. Kouassi Konan Edouard, and the Deputies of their respective universities, for their support. I am indebted to the Coordinator and Scientific Coordinator of the H2 program of Cote d'Ivoire for their contribution to my academic journey. I am truly grateful to my supervisor, Fassinou Wanignon Ferdinand, of the university of Felix Houphouet-Boigny of Côte d'Ivoire for his guidance and mentorship, and my Co-supervisor Prof. Harrie-Jan Hendricks -Franssen, from the Institute of Georesources and Materials Engineering, Faculty Agrosphere (IBG3), Forschungszentrum Julich. I would like to acknowledge the jury members of the University of Felix Houphouet-Boigny Abidjan, Côte d'Ivoire for their valuable insights and feedback on my work. Special thanks go to Dr. Yan Liu from the Institute of Georesources Germany, for his supervision and facilitation during my research in Germany. I cannot overstate my gratitude to my parents Cllr. Nelson S. Jallah and Mrs. Vectorial T. Yelegar, as well as my two brothers, Mr. Momo G. Jallah Sr. and Mr. Nelson S. Jallah Jr., and their wives. Their continuous encouragement and unwavering support were instrumental in the completion of this work.

I would also like to express my appreciation to my colleagues at all four universities, and most importantly, to the two semesters we spent together in Niger, thanks to all of you who provided me with valuable information and assistance regarding my studies.

In conclusion, I would like to extend my heartfelt thanks to everyone who participated in my academic journey. Your support, guidance, and encouragement are invaluable and I am truly grateful. Thank you all.

ABSTRACT

The impact of changing climate on the potential streamflow for hydropower generation is a critical concern in Africa, specifically in the Genale Dawa III(GD-3) catchment in Ethiopia. This study aims to contribute to the growing body of knowledge regarding climate change, streamflow analysis, and hydropower potential in the region. Its aim is to establish a relationship between streamflow and hydropower potential, analyze how climate change affects annual hydropower potential, investigate the impact of climate change on streamflow. Climate change has global implications, directly affecting precipitation, temperature, and streamflow patterns, ultimately impacting the streamflow. Africa, which has abundant hydropower potential, is facing increasing climate hazards.

This study utilized climate data (historical 1996-2005, projected periods 2011-2100) and streamflow data1980-2015. Three climate models, CanESM_RCA4, CSIRO-Mk3-6-0_RCA4, and NorESM_RCA4, under emission pathway RCP 8.5, were incorporated to capture changes in hydropower potential and a range of climate uncertainties. Hydrological simulations were performed (Liu & Olarinoye, 2023). using the HBV model. Additionally, a consistent trend of increasing long-term average temperature and precipitation was observed across all three climate models across the catchment area as 22°C increase until 2100, 1389mm/yr decrease in precipitation. Furthermore, the long-term average streamflow projected a general decrease of 15.7%. The research also assesses the general change of the average long-term change in hydropower potential of the future periods of 34% decrease catchment.

An overall understanding of the potential changes in precipitation, temperature, streamflow, and hydropower generation is crucial in Africa, particularly in the Genale Dawa III catchment. These findings contribute to the assessment of the impact of climate change on hydropower generation and can inform sustainable energy management strategies in the region.

Keywords: (Climate Change, Climate Change Impact, Streamflow, Potential Hydropower, Hydropower Generation, Africa)

RÉSUMÉ EN FRANÇAIS

L'impact du changement climatique sur le débit potentiel des cours d'eau, visant à pour la production d'énergie hydroélectrique, est une préoccupation majeure en Afrique, en particulier dans le bassin versant de Genale Dawa III (GD-3) en Éthiopie. Cette étude vise à l'amelioration des connaissances concernant le changement climatique et l'analyse du débit des cours d'eau et le potentiel hydroélectrique dans la région. L'objectif de ce travail est d'établir une relation entre le débit et le potentiel hydroélectrique, d'analyser comment le changement climatique affecte le potentiel hydroélectrique annuel et d'étudier l'impact du changement climatique sur le debit des cours d'eau. Le changement climatique a des implications globales, affectant directement les précipitations, la température et les caracteristiques d'écoulements fluviaux, ce qui a finalement un impact sur le débit des cours d'eau. L'Afrique, qui dispose d'un potentiel hydroélectrique importan t, est confrontée à des risques climatiques croissants.

Cette étude a utilisé des données climatiques (historiques 1996-2005, scenarios futuristes 2011-2100) et des données sur le débit des cours d'eau couvrant la periode 1980-2015. Trois modèles climatiques, CanESM_RCA4, CSIRO-Mk3-6-0_RCA4 et NorESM_RCA4, sous la trajectoire d'émission RCP 8.5, ont été incorporés pour capturer les changements concernant le potentiel hydroélectrique et une gamme d'incertitudes climatiques. Des simulations hydrologiques ont été réalisées (Liu et Olarinoe, 2023) à l'aide du modèle HBV. En outre, une tendance cohérente à l'augmentation de la température et des précipitations moyennes à long terme a été observée dans les trois modèles climatiques sur l'ensemble du bassin versant: augmentation de 22°C jusqu'en 2100, diminution des précipitations de 1389 mm/an. En outre, le débit moyen à long terme des cours d'eau a enregistré une baisse générale de 15,7 %. La recherche évalue également le changement général de la variation moyenne à long terme du potentiel hydroélectrique des périodes futures de 34% de diminution du bassin versant.

Une compréhension globale des changements potentiels dans les précipitations, la température, le débit et la production d'énergie hydroélectrique est cruciale en Afrique, en particulier dans le bassin versant de Genale Dawa III. Ces résultats contribuent à l'évaluation de l'impact du changement climatique sur la production d'énergie hydroélectrique et peuvent aider à la mise en place des strategies de gestion durable de l'énergie dans la région.

Mots clés:(changement climatique, impact du changement climatique, débit des cours d'eau, potentiel hydroélectrique, production d'hydroélectricité, Afrique)

LIST OF ACRONYMS

TABLE OF CONTENTS

LIST OF TABLES

LIST OF FIGURES

GENERAL INTRODUCTION

GENERAL INTRODUCTION

Climate change remains one of the most pressing challenges confronting humanity in the 21st century. As defined by the United Nations Framework Convention on Climate Change (UNFCCC), climate change refers to alterations in the global atmosphere attributed directly or indirectly to human activities. Human-driven changes can manifest as shifts in precipitation, temperature, and evapotranspiration, all of which play crucial roles in the hydrological cycle. Within these cycles, streamflow holds particular significance.

Given its pivotal role, streamflow significantly affects hydropower generation, making it a subject of critical interest. Unfortunately, Africa, a continent facing various climate hazards, is projected to experience increasing challenges in the 21st century, which could further exacerbate the difficulties in hydropower generation (IEA 2020). Thus, the potential impact of changing climate on streamflow for hydropower generation in Africa is a major concern.

The ramifications of climate change are far-reaching and affect the global ecosystem, leading to events such as floods, droughts, heat waves, cold spells, and even the melting of crucial glaciers, such as those in the Himalayas(Wan et al., 2020). Therefore, it is essential to research and comprehend the implications of climate change on streamflow and its subsequent impact on hydropower generation in Africa. The objectives of this study were to investigate the relationship between streamflow and hydropower potential, analyze how climate change affects the annual hydropower electricity generation potential, and investigate the impact of climate change on the seasonal hydropower potential in Africa and Genale Dawa III(GD-3) in Ethiopia. This research endeavors to employ methodologies for the collection of climate and streamflow data using Python. Through simulation and validation, data from various climate scenarios (CanESM_RCA4, CSIRO-Mk3-6-0_RCA4, NorESM_RCA4) were analyzed, specifically focusing on temperature, precipitation, streamflow, and hydropower potential. These analyses will provide valuable insights into the impact of changing climate on streamflow's potential for hydropower generation in Africa.,

This research aims to contribute to the growing body of knowledge on climate change, streamflow dynamics, and hydropower generation. By understanding the complexities of these relationships, policymakers and stakeholders can be better equipped to develop strategies to mitigate the negative effects of climate change and ensure sustainable energy generation in Africa.

Problem Statement

Climate change poses a significant challenge in the 21st century with implications for various ecosystems and human activities. The United Nations Framework Convention on Climate Change (UNFCCC) defines climate change as an alteration in the composition of the global atmosphere, directly or indirectly attributed to human activities. These activities can lead to changes in precipitation temperature, and evapotranspiration, impacting streamflow a critical component of the hydrological cycle

Africa, a continent with rich hydropower potential, is projected to face increasing climate hazards in the 21st century, potentially challenging hydropower generation (IEA2020). However, the precise impact of climate change on streamflow and its implications for hydropower potential remain a major research question. Climate change-induced events, such as floods, droughts, heat waves, and rising temperatures, further exacerbate the situation(Wan et al., 2021).

This situation demands urgent attention because failure to address these challenges promptly may lead to a significant decrease in Africa's hydropower generation potential. To address this concern, this research aims to investigate the impact of changing climate on the streamflow potential for hydropower generation in Africa, considering future scenarios. The results from the findings will be use to provide crucial insights for sustainable energy planning, water resources management, and climate adaptation strategies in the region.

Research gaps and questions

Africa is vulnerable to the impacts of the Changing Climate on streamflow for potential hydropower generation. There are many studies that have been conducted on this topic, but limited research has specifically focused on the African Context. This study aims to fill this gap by assessing the impact of climate change on streamflow, and thus on hydropower, to establish the relationship between streamflow and hydropower, and to analyze how climate change affects annual and monthly hydropower generation. We assess the impact of climate change on streamflow for the potential hydropower of the Geale Dawe III (GD-3) in Ethiopia.

This study sought to answer the following questions:

- What are the relationships between streamflow and hydropower generation?
- What are the impacts of climate change on streamflow?

- What are the impacts of climate change on hydropower production?

Research hypothesis

The impact of climate change might result in a consequential decrease in streamflow, thereby affecting potential hydropower generation (Wan et al., 2021). This hypothesis suggests that climate change has a negative effect on streamflow, leading to a reduction in the amount of water available for hydropower generation. In this research, the hypothesis assumes that as the climate changes, altering precipitation patterns and temperature regimes, the streamflow in the affected regions will decline. This, in turn, will affect the capacity to generate hydropower, as it relies on a consistent and sufficient supply of water. This hypothesis requires further research and analysis to investigate the specific impacts of climate change on streamflow and hydropower generation in Africa. The hypothesis needs to be tested using appropriate data collection, statistical analysis, and modelling techniques to draw meaningful conclusions.

Research objectives

The overall objectives of this study were to assess the impact of climate change on the potential streamflow for hydropower generation in the Geale Dawe III(GD-3) and to understand how climate change may influence the availability of water resources in the Geale Dawe River basin and consequently impact the potential hydropower generation capacity of the GD-3 River basin. This study had the following key objectives.

- establish the relationship between streamflow and hydropower potential,
- analyze how climate change affects the annual hydropower electricity generation,
- investigate the impact of climate change on the seasonal hydropower potential.

CHAPTER I:
BIBLIOGRAPHICAL REVIEW

Chapter I: BIBLIOGRAPHICAL REVIEW

Introduction

This literature review presents an overview of the impact of climate change on streamflow and hydropower generation, specifically focusing on the relationship between streamflow and hydropower generation, projecting climate change in Africa, assessing the impact climate change has on streamflow and hydropower in Africa.

1. Projected climate change in Africa

Africa is projected to experience increasing climate hazards for the remainder of the 21st century, to minimize these adverse effects of climate change, hydropower needs to enhance Africa resilience to climate change (IEA 2020)

(Larbi et al., 2022) stated that climate change poses a significant threat to water security, particularly in areas that are already facing challenges, such as the Tano River Basin in Ghana. The aim of their study was to assess the projected changes in rainfall and temperature and their impact on streamflow and evapotranspiration in the Tano River basin from 2021 to 2050, compared to the period 1986-2005. Their analysis focused on two Representative Concentration pathway (RCP4.5 and RCP8.5). Their findings revealed that under the RCP4.5 scenario, the main annual rainfall of 1401.9 mm is projected to slightly increase by 0.5% but with a decreasing trend of 1.22 mm/year. Under the RCP 4.5 scenario, the mean annual rainfall is expected to decrease by 3.2% with a decreasing trend of 0.3 mm/year under the RCP8.5 scenario. The annual temperature is projected to increase by 2.1% under RCP 4.5 and RCP 8.5, with statistically increasing trends of 0.07 °C year and 0.09 °C year, respectively.

Their study indicated that the mean annual streamflow is expected to decrease, with a more pronounced decrease of 37.5% under RCP 8.5, compared with a decrease of 19.9% under RCP4.5. Their findings highlight that the projected change suggests a future scenario of altered rainfall patterns, increased temperature, and reduced streamflow as a result of climate change in the region.

Cáceres et al. (2022) stated that climate change can affect hydropower operation through changes in the timing and magnitude of precipitation patterns and increases in evapotranspiration due to rising temperatures. Thus, the IEA (2020) report on climate change on African hydropower projections that the decrease in the region mean hydropower capacity

factor may generate false impressions regarding future climate impacts on African hydropower generation. They concluded that climate change and different levels of global warming will have insignificant effects on future hydropower capacity factors. The report highlighted that climate impact will be largely affected by the level of GHG concentration, but the large decrease in the hydropower capacity factor will be offset by a higher increase in Nile basin countries.

De Oliveira et al. (2017) investigated the effects on the hydropower behavior of the region of the Granda river basin, and the potential hydropower generation from three facilities installed in a cascade within the area. They applied the SWAT model driven by the RCMS Eta-HadGEM2-ES and Eta-MIROC5 to simulate the hydropower potential under the influence of Representative Concentration Pathways (RCP) 4.5 and 8.5. In their simulation, the SWAT model was calibrated and found in a validation study to reproduce the natural streamflow for the baseline period from 1961-2005. Their findings indicated significant reduction in streamflow and consequently in runoff during all simulation periods and for all radiative forcing scenarios compared to the baseline period.

1.1 Impact of climate change on streamflow

Numerous studies have investigated the impact of climate change on streamflow. The review examines the impact of climate change on streamflow in various regions. Several studies were reviewed, and highlighted the effects of climate changes on streamflow. These various studies reveal the impact of climate change on streamflow reduction which leads to decreased energy generation and hydropower generation (chen et al.,2016). For instance, Chen et al. (2016) conducted a study in the United States and highlighted that climate change-induced runoff reduction would result in decreased energy generation and revenue hydropower plants operating in the Columbia River and California systems. Moreover, prolonged rainfall events were found to significantly influence the runoff regime, particularly during the growing season and periods of snowmelt.

Zheng et al. (2009) observed a substantial decrease in streamflow in the Yellow River region (Zheng et al., 2009) since the 1990s. Specifically, they reported a decrease of up to 65% compared with the average streamflow values from the 1950s to the 1990s. At one hydrologic station along the Yellow River, zero flow was observed at Lijun station for 226 days in 1997.Wang et al. (2008) further revealed that climate change accounted for 43-75% of these occurrences of zero flow. Additionally, Liu et al. (2019) and ; Liu and Zhang (2004) found that streamflow in the upper reach of the yellow river decreased by 5.75 billion m^3/ year (around

16.5%) when comparing the 1990s to the period of the 1950s-1960s. This reduction was primarily attributed to the reduced precipitation, which accounted for 75% of the observed decrease. Similarly, in the reach of the Yellow River, streamflow decreased by 63.1 billion m^3/ year (21.8%), with climate changes accounting for 43% of the observed reduction Furthermore, studies have suggested that climate changes can lead to an increase in evapotranspiration (ET) and a decrease in runoff by 5.7-24%. Additionally (Kankam-Yeboah et al., 2013) conducted a study on the impact of climate change on streamflow in selected river basins in Ghana. They estimated the impact of climate change on the streamflow in the White Volta River. They used the SWAP method to estimate climate projections of annual streamflow for the 2020s (2006-2035) and the 2050s (2036-2075). Their analysis showed for (2006 -2035) a decrease of annual streamflow of 22 and 50%, 22 and 46% respectively. They concluded by stating that there is a need to put in place appropriate adaptation measures to foster resilience to climate change. Sirisena et al. (2021) also utilized the Soil Water Assessment Tool to assess streamflow and sediment patterns in the Irrawaddy River Basin for two timeframes: 2046–2065 and 2081–2100. They examined RCP 2.6 and RCP 8.5 climate scenarios, both with and without planned reservoirs. Climate change alone led to substantial mid- and end-century increases in streamflow (8–45%) and sediment loads (13–75%) at the basin outlet. Reservoir inclusion showed a minor impact on streamflow but reduced sediment loads by 4–6% under RCP 8.5 in the century. Seasonally, reservoirs lowered monsoon streamflow by 6–7% and raised non-monsoon flow by 32–38%, while sediment load would decrease by 9–11% in monsoon periods and rise by 32–44% in non-monsoon times. The reviewed studies collectively demonstrate the detrimental impact of climate change on streamflow in different regions. Reduction in precipitation, combined with increased evapotranspiration, contribute to decreased streamflow, While the existing evidence provides valuable insights, there are several research gaps that need to be addressed in the African scenarios. A deeper understanding of the mechanisms through which climate change impact streamflow patterns is necessary to be addressed in the African context.

Overall, the reviewed studies demonstrate the detrimental impact of climate change on streamflow in various regions, resulting in reduced hydropower generation. However, there are research gaps that need to be addressed, particularly in the African context. Furthermore, understanding of the mechanisms through which climate change affects streamflow patterns is necessary for effective adaptation measures.

1.2 Impact of climate change on hydropower

Hydropower, is a vital renewable energy source, It is susceptible to the impact of climate change. (Beheshti et al., 2019). Assessing the potential of hydropower under changing climate conditions is an area of active research. This part of the literature review examines the climate change impact on hydropower.

Hydropower accounts for close to 16% of the world's total power supply and is the world's most dominant (86%) source of renewable electrical energy, and depends on streamflow and therefore on precipitation for power generation (Hamududu and Killingtveit, 2012).

Chen et al. (2016) further stated that global warming has the potential to disrupt the water cycle, thereby influencing the availability and distribution of hydropower resources across the regions. Freitas & Soito (2009) conducted a study in Brazil, and demonstrated that increasing global warming could impact the hydrological cycle and subsequently affect hydropower resources in the country. Such findings underline the importance of understanding the impact of climate change on the water cycle and its consequences for potential hydropower generation. Moreover, rainfall and temperature are crucial factors affecting hydropower generation. Liu et al. (2016) have reported significant link between climate change and hydropower generation. They stated that an increased in rainfall positively correlates with hydropower generation, as it leads to higher runoff and water storage in reservoirs, thereby promoting hydropower production. They further indicated that rising temperature directly impact hydropower by reducing the storage capacity of reservoirs, limiting generation potential. Vliet et al. (2016) have conducted comprehensive assessments of hydropower potential in various river basin. Their studies evaluated the impact of climate change on hydropower generation and provided valuable insights into the vulnerability and sensitivity of the hydropower system to climate fluctuations. Additionally, (Fan et al., 2020) highlighted the existence of regional differences in China by the impacts of climate factors on hydropower generation. An econometric model for regional hydropower generation of 15 were constructed to explore the impact of climate factors on hydropower generation in different 16 regions of China by using the monthly panel data of 28 provinces in China caused by the changes 18 of climatic factors under the three climate change scenarios (RCP2.6, RCP4.5 and RCP8.5) Their research also reveals the sensitivity and vulnerability of hydropower to climate fluctuation, introducing uncertainties for its development. They further stated that climate change can either increase or decrease streamflow, adding complexity to the hydropower forecast. The regions with abundant

hydropower resources may be particularly susceptible to the impacts of climate change, emphasizing the need for adaptive strategies and robust planning. Nonki et al.(2021) conducted research on the Lago dam, Benue River basin, northern Cameroon. Their objective was to investigate the impact of climate change on the hydropower potential of the dam. To achieve this, they employed the HBV-Light hydrological model, coupled with dynamically downscaled temperature and precipitation data from the REMO regional climate model. Their findings of the study revealed that future climate change scenarios, characterized by increased precipitation and streamflow, as well as elevated potential evapotranspiration (PET), are expected to have a detrimental effect on the hydropower potential of the Lagdo dam. The combined influences of these factors indicate a decrease in the efficiency and productivity of the dam's hydropower generation. Their study shows the importance of considering climate change impacts when assessing the sustainability and long-term viability of hydropower projects.

Based on the past studies the literature review confirms that climate change significantly affects hydropower resources and generation. Global warming disrupts the water cycle, leading to changes in the availability and distribution of hydropower resources in Africa. Rainfall also plays a crucial role in promoting hydropower generation, while rising temperature and precipitation directly impact reservoir storage capacity. The higher rainfall positively correlates with hydropower generation by increasing runoff and water storage in reservoirs, thereby promoting production. However, rising temperature directly impact hydropower by reducing reservoir storage capacity and limiting generation potential. Assessing hydropower potential under climate change is an ongoing research area in Africa, because there is limited research in the Africa context, with regional differences highlighting the vulnerability of hydropower system to climate fluctuations.

Climate change impacts are crucial when assessing the sustainability and long-term viability of hydropower projects. However, there is a limited amount of research of this topic in Africa, and in order to further understand and address the impacts of climate change on hydropower resources in Africa more study is needed.

1.3 Relationship between streamflow and hydropower generation

The relationship between streamflow and hydropower generation is a pivotal aspect of water resources management and energy production. Various methodologies have been developed to understand and quantify this intricate connection. In this section, we employed various approaches to establish the relationship between streamflow and hydropower generation. These

approaches include the customized approach method, the power-discharge relationship method, the power elevation relation method, and the method for quantifying hydropower electricity.

(1) Customized approach method

The relationship between streamflow and hydropower generation can be determined by the water level, streamflow volume, and water velocity De Oliveira et al.(2017) discuss streamflow and potential hydropower generation as the maximum amount of power that can be generated based on the total plant efficiency, streamflow and hydropower heard. Their definition linked the relationship between streamflow and hydropower generation. They applied the mathematical equation below that relates various variables of streamflow and hydropower generation in Equation (1)

$$P_t = Q \times H \times \rho_w \times g \times n \quad (1)$$

Where P_t is the hydropower potential (w); Q is the streamflow (m^3s^{-1}); H is the hydraulic head (m); ρω is the water density (kgm^{-3}); g is the gravitational acceleration (ms^{-2}) and n is the total plant efficiency.

The customized approach method is used to calculate the potential hydropower generation by using the time series obtained from the water balance model, to calculate the monthly future usable capacity. The method quantifies the hydropower output for hydropower dams and for runoff hydropower structures. The major input variables require time series of Q and H. Somehow, to obtain H, extra info or methods are needed. Cáceres et al. (2022) used this method to analyze hydropower usable capacity and variability.

(2) Power-Discharge Relationship Method

Sieber et al. (2005) discussed the power discharge relationship (flow duration curve) as the cumulative frequency distribution of streamflow values over a specified period. The FDC was used to estimate the relationship between streamflow and hydropower generation. Equation (2) relates streamflow (Q) and power generation (P) using the flow duration curve

$$P = K * Q^m \quad (2)$$

Where:

P is the hydropower generation (kW), Q is streamflow(m^3s^{-1}) and K is a constant, m is an exponent, often referred to as the efficiency exponent or head -flow exponent. The value of k and m can be determined empirically on historical data or through system specific studies

Sieber et al. (2005) used this method to analyze the relationship between streamflow and hydropower generation. They applied the method by plotting the flow duration curve (FDC), which represents the cumulative frequency distribution of streamflow value over a given period of their study.

(3) Power- Elevation Relationship Method

(Nonki et al., 2021) used the power elevation relationship method of the head- flow curve to describes the relationship between the hydraulic head (H) and flow rayed (Q). It is typically derived from physical measurements of the hydraulic model. They relate hydropower generation (P) and streamflow (Q) using the head- flow curve according equation 3

$$P = k * Q * H \quad (3)$$

where

P is the hydropower generation (kW), Q is streamflow (m^3/s). H is the hydraulic head (the difference in elevation between the upstream and downstream water levels) (m), k a constant. The value of k depends on the specific characteristics of the hydropower system, such as turbine efficiency, generator efficiency, and transmission losses.

(4) Quantifying the amount of hydropower electricity

The amount of hydropower electricity HP_t (kWh) produced over a time period H_t can also be quantified using the following Equation (3) (El-Hawary & Christensen, 1979; Wan et al., 2020; Zhao et al., 2014)

$$HP_t = min(\eta . Q_{t,turb}\, H_t, N_{installed}) . \Delta t \quad (4)$$

Where η is a comprehensive hydropower coefficient (kN/m^3) that combines gravitational acceleration (m s^{-2}) and density of water (kg m^{-3}), $Q_{t\ trub}$ is the rate of water flow through a pipe and turbine (m^3/s), H_t is hydraulic head with respect to the outlets of the pipe(m), that is the difference between elevations of forebay and tailwater, and $N_{installed}$ is the installed capacity of the power plant ($kW=kJs^{-1}$), that is the maximum power output that can produced by a specific plant.

PARTICAL CONCLUCION

The selection of an appropriate method for analyzing the streamflow and hydropower relationship is crucial in assessing the potential impacts of changing climate conditions on hydropower generation. In this study, we have opted for the customized approach method (Eq1), which offers a versatile framework for estimating hydropower potential by taking into account a range of variables ($P_t = Q \times H \times \rho_w \times g \times n$). This method proves particularly advantageous when evaluating the influence of climate-related factors such as precipitation patterns, temperature changes, and streamflow alterations. While alternative methods like the Power Discharge Relationship Method, Power-Elevation Relationship Method, and Quantifying the Amount of Hydropower Electricity Method each hold their own merits and find valuable applications in specific contexts, the customized approach method emerges as the most suitable choice for our investigation. Given the diverse climate conditions and potential hydropower opportunities in Africa, the customized approach method provides a comprehensive and tailored approach, allowing for the incorporation of multiple factors that influence hydropower generation. This ensures a robust assessment of the impact of changing climate on streamflow and subsequent hydropower potential in the region.

CHAPTER II:
MATERIALS AND METHODS

Chapter II: MATERIALS AND METHODOLOGY

Introduction

This chapter presents the method that was used to collect and analyze data for this study. It also presents the study area, data, hydrological model, model description and model setup

1. Study area

This study was conducted in the catchment of the Genale Dawa III(GD-3)., which is located in southeastern Ethiopia. The basin covers a portion of the Southern Nations, Nationalities, and Peoples (SNNP), Oromia, and Somali regional states. The basin covers an area of approximately 172,713 km^2. It is one of Ethiopia's three widest river basins specifically, the upper Genale River basin(Shigute et al., 2022).

The catchments study area is located between the latitudes of 6°52′ and 5°20′ N and longitudes of 38°30′ and 39°45′ E, and lies in the upper central area of the basin. Owing to topographic and inter-tropical convergence zone (ITCZ) effects, the basin experiences bimodal type I (three seasons) and bimodal type II (double wet and dry seasons) annual rainfall cycles in the northern (highland) and southeastern (lowland) regions, respectively. The northern and highland area is characterized by three wet seasons, March–May (locally known as belg), June–September (locally known as kiremt), and September–November (locally known as meher) The lowland and the southeastern parts of the study area experience two wet seasons, one from March to May, with the highest precipitation in April, and the other from September to November, with the highest precipitation in October. The annual average rainfall varies from 161.8 mm to 591 mm. The annual mean minimum and maximum temperatures range of the GD-3 catchment is between 6.9 and 16.2 °C and 18.9–27.7 °C, respectively.

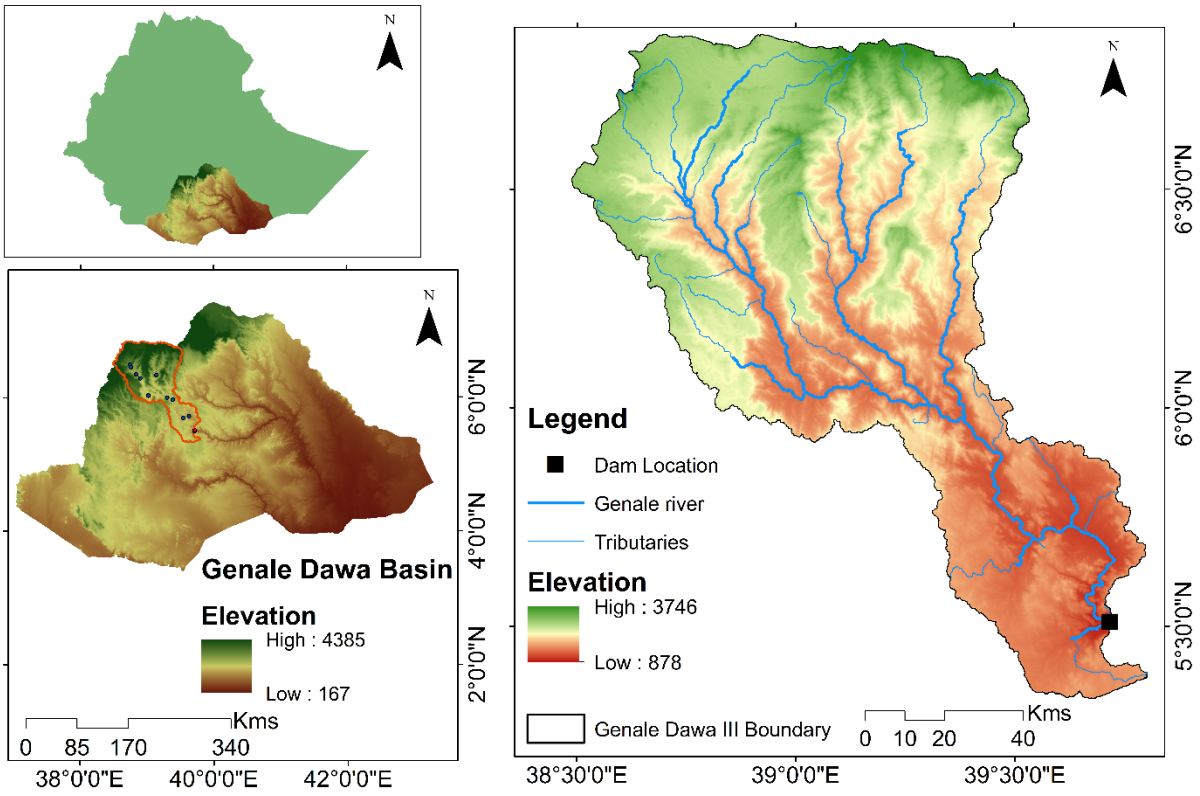

Figure 1: Study area of the Genale Dawa River III (GD-3) in Ethiopia (Abraham, 2023).

The dam (Fig.2) is located in the study area of Genale Dawa III(GD-3) in Ethiopia. The pacific site of the dam is located in a low seismic hazard area of class I. The dam is 110m high, 456m wide and 450m long, with a volume of 3.2million cubic meters (Mm^3). At the full capacity the dam can store up to 2570$Mm^3$of water. The net head of the dam is 273m. When the GD-3 dam is completed it will have a total installed generating capacity of 254MW, with three functioning vertical Francis's turbine generators, each having a generating capacity of 84.7MW.

Figure 2 : GD-3 dam(https://infrastructurebrief.com/ethiopia-completes-construction-of-genale-dawa-iii-dam

2. Data

Climatic projections are from three climate models CanESM_RCA4, CSIRO-Mk3-6-0_RCA4 and NorESM_RCA4. The data were collected by the Institute of Earth and Environmental Sciences Ethiopia, the data was used for the study area of the Genale Dawa III(GD-3) in Ethiopia.

The period of data collected for the simulation was for the historical period 1996-2005, and for the projected period 2011-2100 respectively, because of the highest data availability. Three scenarios (Near future, Future and Far future 2011-2100) for both climatic data and streamflow data (1996-2015), were chosen. The data collection procedure takes local climatic data into account, and streamflow data at a resolution of 0.1°(MSWEP Dataset), and 0.44°(CanESM_RCA4, CSIRO-Mk3-6-0_RCA4, NorESM_RCA4.) of the climatic data and the resolution daily data for streamflow .

The table below provides details about the Data, Parameter, Data Source, Time Range, Resolution, and References utilized for the data analysis. The variables encompass climate data

such as temperature and precipitation for both the historical period (1996-2005) and the projection period (2011-2100). The data source for climatic data is MSWEP with a resolution of 0.1°, and CanESM_RCA4, CSIRO-Mk3-6-0_RCA4, and NorESM_RCA4, with resolutions of 0.44°. Additionally, time series of streamflow data were available for the historical period of 1980-2015, at daily resolution.

Table 1 : Presentation of Climatic Forcing (historical and projection period) and Streamflow data (Time series)

Data	Parameters	Data Source	Time Range	Resolution	References
Climate Forcing	Precipitation Historical	MSWEP Dataset	1996-2005	0.1°	https://www.gloh2o.org/mswep/
	Projection Period)	CanESM_RCA4, CSIRO-Mk3-6-0_RCA4, NorESM_RCA4	2011-2100	0.1°	https://www.gloh2o.org/mswep/
	Temperature (Historical & Projection Period)	CanESM_RCA4CSIRO-Mk3-6-0_RCA4, NorESM_RCA4 3GCMs (Cordex)	1996-2005 2011-2100	0.44◦	https://confluence.csiro.au/public/CSIROMk360 https://cordex.org/domains/cordex-domain-description/ -019-04974-z https://cordex.org/
	PET (Historical & projection Period	CanESM_RCA4 CSIRO-Mk3-6-0_RCA4, NorESM_RCA4 GCMs (Cordex)	1996-2005 2011-2100	0.44◦	https://confluence.csiro.au/public/CSIROMk360 Africa: https://cordex.org/domains/cordex-domain-description/
Streamflow	Historical	Time series	1980-2015	Daily Data	Genalie chenemasa station

3. Overall workflow

The figure shows the overall workflow of the HBV model. The relationship between streamflow (Q) and hydropower potential (Pt) for a historical period and a projected period. The figure also shows the impact of climate change on potential hydropower and the uncertainty associated with these projections.

Overall workflow

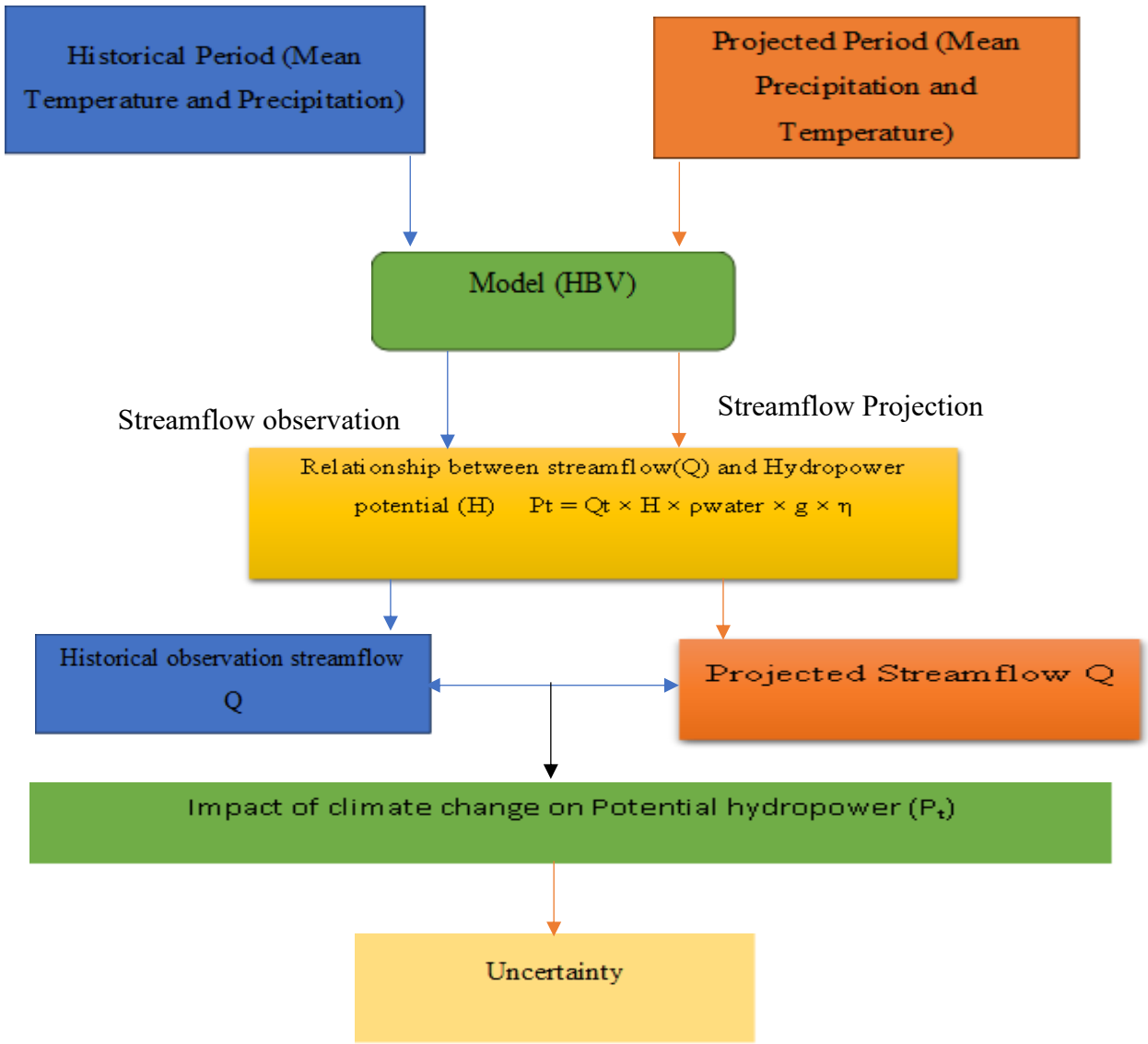

Figure 3: overall flowchart showing the concept of analysis

4. Hydrological Modelling

Hydrological models (precipitation-runoff-models) deal with the relationship of water in the environment, investigating the occurrence, circulation and distribution of water within each phase of the hydrologic cycle (Bergström & Forsman, 1973). Moreover, these models consider the chemical and physical properties of water and the interaction with the environment. Due to land cover changes, increasing urbanization, industrialization and deforestation, various changes have occurred in hydrologic systems around the world. Climate change as well as soil heterogeneity also have a direct impact on the discharges of many rivers (Bergström, 1976a). Today there is a big variety of different hydrological models available to analyze these relations. These models are used for the modelling of both gauged and ungauged catchments. Each model has its own unique characteristics. The inputs used by different models are rainfall, air temperature, soil characteristics, topography, vegetation, hydrogeology and other physical parameters. All these models can be applied in very complex and large basins. The results help to manage flood forecasting, water distribution, evaluation of water quality, erosion, sedimentation, land use changes, nutrient and pesticide application as well as the impact of climate change scenarios (Devia et al., 2015).

In this study we used the HBV model of Bergström (1976) which has been applied in a wide range of climate and hydrological conditions (Seibert & Vis 2012). The HBV model has been tested in various parts of the world and was frequently applied in several regionalization studies due to the simplicity and flexibility of its model structure (Seibert, 1999)

The HBV model was used to simulate discharge by considering various input parameter. To represent evapotranspiration and recharge processes, the soil moisture routine as outlined by Beck et al. (2020) was integrated in to the model. The regionalized parameters for the HVB model were obtained.

4-1 Schematic structure of HBV model

The schematic structure of the HBV model shown in figure(4) is a semi-distributed hydrologic model used to simulate catchment runoff. The model consists of several components that simulate different hydrological processes. The abbreviations of the schematic structure model shown in figure(4) prepresent different parameters in the model. These abbreviations include temperature (T), snowfall correction factor (CFMAS), snowfall (SF), water holding capacity of snow (CWH), rainfall correction factor (CFR), upper zone recession coefficient (K0), lower

zone recession coefficient (K1), baseflow recession coefficient (K2), upper zone storage limit (UZL), percolation rate from upper to lower zone (PERC), field capacity of soil moisture storage (FC), wilting point of soil moisture storage (LP), shape coefficient for lower zone storage outflow (BETA), and maximum baseflow rate (MAXBAS).

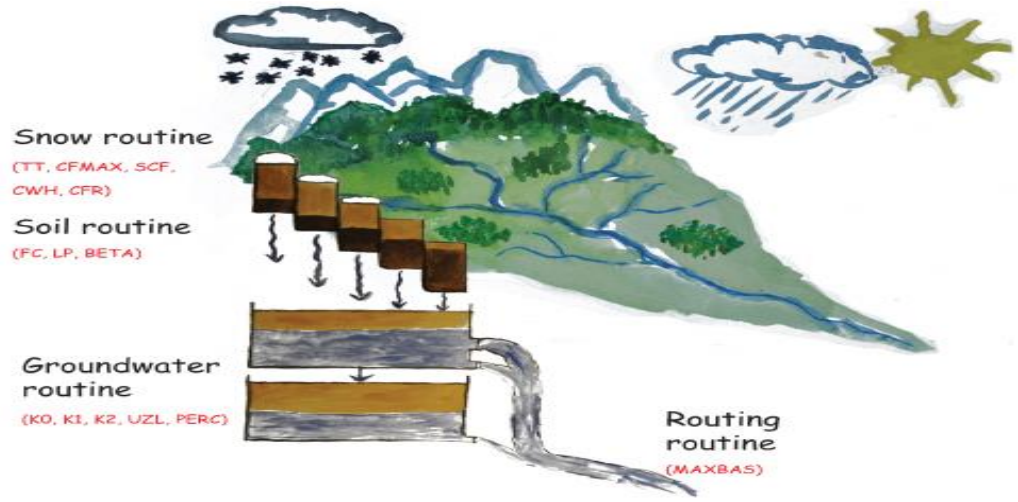

Figure 4: Schematic structure of the HBV model

4-2 Model description

The HBV hydrological model is used to analyze river discharge and water pollution. It is a rainfall-runoff model, which includes conceptual numerical descriptions of hydrological processes at the catchment scale. In this model, the general water balance can be described according (Bergström & Forsman, 1973):

$$P - E - Q = \frac{d}{dt}[SP + SM + UZ + LZ] \qquad (5)$$

where

P = precipitation(mm), E = evapotranspiration(mm), Q = runoff (m^3/s), SP = snow pack (mm), SM = soil moisture (L), UZ = upper groundwater zone (m), LZ =lower groundwater zone (m)

The model consists of different routines and simulates catchment discharge, usually at a daily time step, based on time series of precipitation and air temperature as well as estimates of monthly long-term potential evaporation rates.(Seibert & Vis, 2012). In this research the model did not take in to account the snow routine as snow plays an insignificant role in the studied catchment. Groundwater recharge and actual evapotranspiration are simulated as function of actual water storage. Also, runoff is computed as a function of water storage. Finally, in the

routing routine a triangu-lar weighting function, is used to simulate the routing of the runoff to the catchment outlet (Beck et al.2020):

$$\frac{F(t)}{I(t)} = \left(\frac{Ssoil(t)}{Pfc}\right) PBETA \quad (6)$$

$$E = Epot.min\left(\frac{Soil(t)}{Pfc.Plp}\right) \quad (7)$$

The model used the above equations (6) to calculate the ratio of actual evapotranspiration (F(t)) to potential evapotranspiration (I(t)). The symbols used, F(t): Actual evapotranspiration, I(t): Potential evapotranspiration, Ssoil (t): Soil moisture storage (mm), Pfc: Field capacity of soil moisture storage (mm) and PBETA: Shape coefficient for lower zone storage outflow.

Equation (7) was also used to calculate is used to calculate actual evapotranspiration (Eact) based on potential evapotranspiration (Epot) and soil moisture storage (Soil(t)). The symbols used: Eact: Actual evapotranspiration (mm),Epot: Potential evapotranspiration (mm), Soil(t): Soil moisture storage (mm),Pfc: Field capacity of soil moisture storage (mm) and Plp: Wilting point of soil moisture storage (mm).

The model also takes into account the Groundwater box ($S_{UZ,}$ mm) P_{PERC} (mm.d^{-1}). The maximum percolation rate from the upper to the lower groundwater box ($S_{LZ,}$ mm). Runoff from the groundwater boxes is also computed as the sum of two or three linear outflow equations ($P_{Ko.}$ P_{K1} and PK2, d^{-1}, depending on whether SUZ is above a thresh-old value, PUZL (mm), This runoff is finally transformed by a triangular weighting function defined by the parameter PMAXBAS to give the simulated runoff (mm.d^{-1}) in equation 8 & 9:

$$\mathrm{QGW(t)} = \mathrm{PK2} \cdot \mathrm{SLZ} + \mathrm{PK1} \cdot \mathrm{SUZ} + \mathrm{PK0} \cdot \max(\mathrm{SUZ} - \mathrm{PUZL}, 0) \quad (8)$$

$$Q_{sim(t)} = \sum_{i=1}^{PMAXBAS} \mathrm{c(i)}.\mathrm{QGW(t-i+1)}$$

where $c(i) = \int_{i-1}^{i} \frac{2}{P_{MAXBAS}} - \left|u - \frac{P_{MAXBAS}}{2}\right| \frac{4}{P_{MAXBAS}^2} \mathrm{du}$ (9)

The long-term mean values of the potential evaporation, Epot, M, for a certain day of the year are corrected to its value at day t, Epot(t), by using the deviations of the temperature, T (t), at a certain day, from its long-term mean, TM, and a correction factor, PCET (−1◦C). This application can be applied in equations (10) (Lindstrom and Bergstrom, 1992).

$$\mathrm{EPOT(t)} = \big(1 + \mathrm{PCET} \,.\, (\mathrm{T(t)} - \mathrm{TM})\big).$$

$$\text{EPOT, M, but } 0 \leq \text{EPOT(t)} \leq 2.\text{EPOT, M} \quad (10)$$

Besides the standard version several alternative model variants can be chosen in HBV. For instance, instead of the two linear outflows from the upper groundwater box, one non-linear outflow can be used in (Eq. 11).

$$Q_{GW(t)=P_{K2}.S_{LZ}+P_{K1}.S_{UZ}^{1+P_{ALPHA}}} \quad (11)$$

4-3 Model setup

The HBV model was setup using as input climate data (historical and projection period), streamflow data taking into account the three climate models CanESM_RCA4, CSIRO-Mk3-6-0_RCA4, NorESM_RCA4. The collection of the data takes in to account the projection time period from 2011-2100, historical time period from 1996-2005 and streamflow data 1980-2015. The parameters of the HBV were calibrated with historical climatic forcing data, observed and streamflow data. The calibration process was performed by (Liu & Olarinoye, 2023).The parameters were adjusted to match the model's simulated streamflow with the observed streamflow. From the calibration the output of the calibrated was used to obtain near-future, future, and far-future climate and streamflow projections from the data. We applied the future climate projections to the calibrated HBV model. The HBV model was used to run the climate scenarios to simulate the future streamflow We analyze the simulated future streamflow to assess the potential impact of changing climate on streamflow. The model compared the future streamflow with historical streamflow patterns. The simulated climate and streamflow data was used to estimate the potential hydropower generation in the catchment area. The model enables us to assess the impact of changing streamflow on the hydropower generation potential. The model quantifies the uncertainties associated with the climate projections, model parameters and calibration process. ((Lindström, et al.1997)

4-4 Function transferring streamflow to hydropower generation

In applying the function transferring streamflow to hydropower generation we used the time series obtained from the water balance model, and calculated monthly future usable capacity. The usable capacity is defined as the maximum monthly capacity in MWh, constrained by the power plant's installed capacity that the simulated streamflow can maintain for a specific time frame(t).

$$P_t = Q \times H \times \rho_w \times g \times n \quad (12)$$

where (Pt) is the power output of the hydropower plant, Q is streamflow, H is the effective height, ρ_w is the water density, ($1000kgm^{-3}$), g is the gravity constant ($9.8ms^{-2}$), and n is the turbine efficiency (90%).

Hydropower potential was simulated in R by (Liu & Olarinoye, 2023). The postprocessing is done by using the required reservoir power plant to simulate water release for which they used the reservoir package as input in to R (Leon et al.1998). This formulation optimizes water releases through a dam by maximizing hydropower generation using maximum velocity of water flow through the turbine (V_{Max}), velocity of water flow through the turbine that is used for power generation, (V_{use}) and the maximum amount of water that can be released through the dam (Max).

4-5 Analysis methods of the change in hydropower generation

The assessment of changes in hydropower generation involves a comprehensive analysis of streamflow data to identify patterns, trends, and influencing factors over time. Various method can be employed to analyze these changes effectively. In this study, the approach proposed by (Xu & Singh, 2005)was adopted, utilizing the HBV model to operate at a specific time scale with mean temperature as an input to calculate potential evapotranspiration (PotET).

The HBV model utilized climate data as input for the catchment. Subsequently, the obtained results were processed using Python to calculate the catchment's streamflow and determine the potential hydropower generation (Pt). The three climate models (CanESM_RCA4, CSIRO-Mk3-6-0_RCA4, and NorESM_RCA4,) were examined to understand the potential changes under varying climate scenarios.

In the study, the essential parameters such as the design flow(Q), reservoir's maximum and usable capacities (Vmax and Vuse), reservoir's maximum area (Amax), and the power plant's effective height(H) to calculate the usable capacity were considered. To analyze reservoir power plants, we harnessed the power of the reservoir package in python, simulating water releases and maximizing hydropower generation using Vmax,Vuse, Amax, and other pertinent parameters, in accordance with the work by (Cáceres et al., 2022).

PARTICAL CONCLUSION

In this chapter two, we have outlined the methodology employed for assessing the hydropower potential and analyzing changes in hydropower generation under varying climate scenarios. The process involved the application of the hydropower generation function ($Pt=Q\times H\times \rho w\times g\times n$) to convert streamflow data obtained from a water balance model into usable capacity, representing the maximum monthly capacity in MWh that the power plant can sustain over a specific time frame. The simulation of hydropower potential was conducted in the R environment, following the methodology proposed by Liu and Olarinoye (2023), and further post-processed using the reservoir package in R as input (Leon et al., 1998). This formulation allowed for the optimization of water releases through a dam, aiming to maximize hydropower generation while considering factors like maximum velocity of water flow through the turbine (VMax), usable velocity for power generation (Vuse), and the maximum release capacity of the dam.To analyze changes in hydropower generation, we adopted the approach introduced by Xu and Singh (2005), which involves the use of the HBV model operating at a specific time scale with mean temperature as an input to calculate potential evapotranspiration (PotET). This model leveraged climate data to compute catchment streamflow and subsequently estimate potential hydropower generation (Pt). We examined three climate models to assess potential changes in hydropower generation under different climate scenarios (CanESM_RCA4, CSIRO-Mk3-6-0_RCA4, and NorESM_RCA4)

Furthermore, key parameters such as design flow (Q), reservoir capacities (Vmax and Vuse), maximum reservoir area (Amax), and power plant effective height (H) were taken into account in the analysis. For the evaluation of reservoir power plants, we utilized the reservoir package in Python, following the methodology outlined by Cáceres et al. (2022), which enabled the simulation of water releases and maximization of hydropower generation using relevant parameters. This chapter establishes a robust framework for assessing hydropower potential and understanding the potential impacts of changing climate conditions on hydropower generation. The methodology outlined here forms the basis for the subsequent analyses and findings presented in the following chapters.

CHAPTER III:
RESULT AND ANALYSIS

Chapter lll: RESULTS AND ANALYSIS

Introduction

This chapter presents a comprehensive analysis of the obtained results, shedding light on the key findings that emerged from the research. The outcomes presented in a structured manner, allowing for a clear understanding of the insights gained from the study.

1.Change in precipitation and temperature

1.1 Change in precipitation

The result of this section presents the changes in precipitation by analyzing the long-term average precipitation, monthly mean precipitation, and annual precipitation of the catchment.

Figure 5 below shows that the three future periods have lower precipitation than that of the historical period. for instance, GCM2 shows a decreasing trend from the historical period to the three future periods. It shows a decrease from 1448mm/yr (historical) to 1323mm/yr(far future). For GCM3, we see higher precipitation in the historical period than in the other three future periods. Generally, the three GCMs have an average of 1420mm/yr in the historical period, and 1408mm/yr, 1375mm/yr, and 1351mm/yr in the three future periods respectively. The relative decrease of precipitation from historical to near future, future, and far future is 0.84%,3.2%, and 4.9%, respectively.

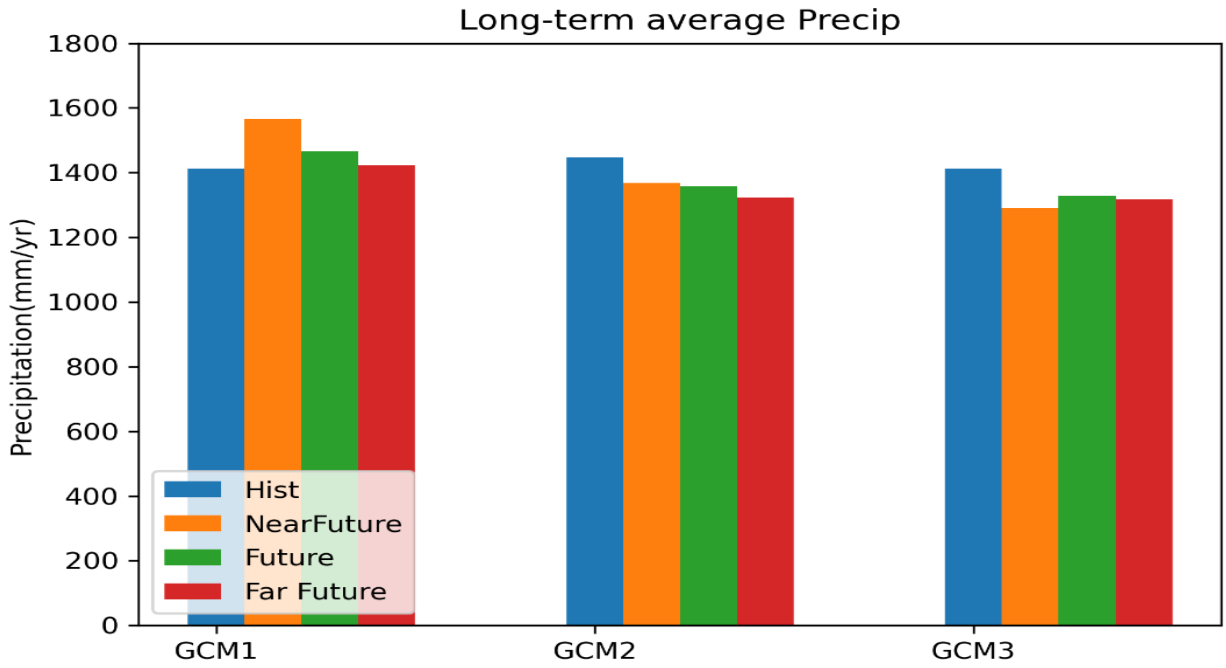

Figure 5 Comparison of GCMs across four time periods of long-term average precipitation values of historical, (1996-2005) and projected periods (near future, Future, and Far future). Long-term average precipitation is calculated as the mean of the daily precipitation over a time period times 365.25.

The table presents the long-term mean projection of precipitation for the catchment area, as simulated by various Global Climate Models (GCMs) across four time period. The table provides insights of variables into how precipitation patterns are expected to change across four distinct time periods as predicted by the GCMs.

Table 2: the long-term mean projection of precipitation across four time periods of GCMs in the catchment

Time periods	GCM1	GCM2	GCM3	Mean
Historical	1400mm/yr	1448mm/yr	1412mm/yr	1420mm/yr
Near Future	1567mm/yr	1367mm/yr	1290mm/yr	1408mm/yr
Future	1447mm/yr	1356mm/yr	1328mm/yr	1375mm/yr
Far Future	1412mm/yr	1323mm/yr	1317mm/yr	1351mm/yr

This analysis from the study examines changes in precipitation patterns over the long term average period of the catchment, considering historical, near future, future, and far future periods. Key observations include comparing long-term average, precipitation for different time periods, including historical data and three future projections. The analysis reveals a general

trend of decreasing precipitation over time, which could impact the streamflow pattern, and hydropower potential with in the catchment. One of the main findings is that all three future periods show lower precipitation levels compared to the historical period. This suggests a general trend of decreasing precipitation over time. This observation is significant as it could have implications on the streamflow pattern and hydropower potential as well as the local water resources, ecosystem, and climate patterns. The analysis involves multiple GCMs, each providing a different projection of future climate conditions. The observed in the study GCM2 and GCM3, shows a consistent decreasing trend across all three future periods, with the far-future period having the lowest precipitation compare to GCM1. This variation between GCMs emphasizes the uncertainty inherent in climate projections and underscores the importance of considering multiple models for a more comprehensive understanding.The analysis provides average precipitation values for each period across the three GCMs. The historical period has an average of 1420mm/yr, and the future periods have decreasing averages: 1408mm/yr for the near future, 1375mm/yr for the future, and 1351mm/yr for the far future.

To quantify the extent of change, the analysis calculates the relative decrease in precipitation from the historical period to the future periods. The near future experiences a decrease of 0.84%, the future period has a decrease of 3.2%, and the far future sees the greatest decrease at 4.9%. These percentages provide a clear understanding of the magnitude of change across the different future time frames.The analysis's implications are crucial for streamflow analysis , water resource management for hydropower potential within the Africa. Decreasing precipitation could lead to low streamflow pattern and low hydropower potential. The differential projections among GCMs highlight the complexity of climate modeling and the need for adaptive strategies that consider a range of possible future scenarios.

In conclusion, the analysis of precipitation patterns based on long-term average, monthly mean, as well as the projections of three GCMs, suggests a consistent trend of decreasing precipitation over the future periods compared to the historical period. While there are variations between the GCMs themselves, the general consensus is that the catchment area can expect reduced precipitation in the coming years. This has potential implications on the reduction of potential hydropower generation in Africa.. The findings emphasize the importance of adapting to changing precipitation patterns and considering these projections in future planning and decision-making processes.

1.2 Monthly mean precipitation

GCM1 indicates that from January to April the precipitation is increasing from historical period to far future period(fig.6). For instance, we see a 2.5mm/day increase from the historical period to the far future period in March. From October to December, we see a decreasing trend. For example, in October the figure highlights a decreasing trend of about 2.3mm/day from historical period to the far future period, and it corresponds to 23% decrease. From May to September there is not a specific trend among the months over the period.

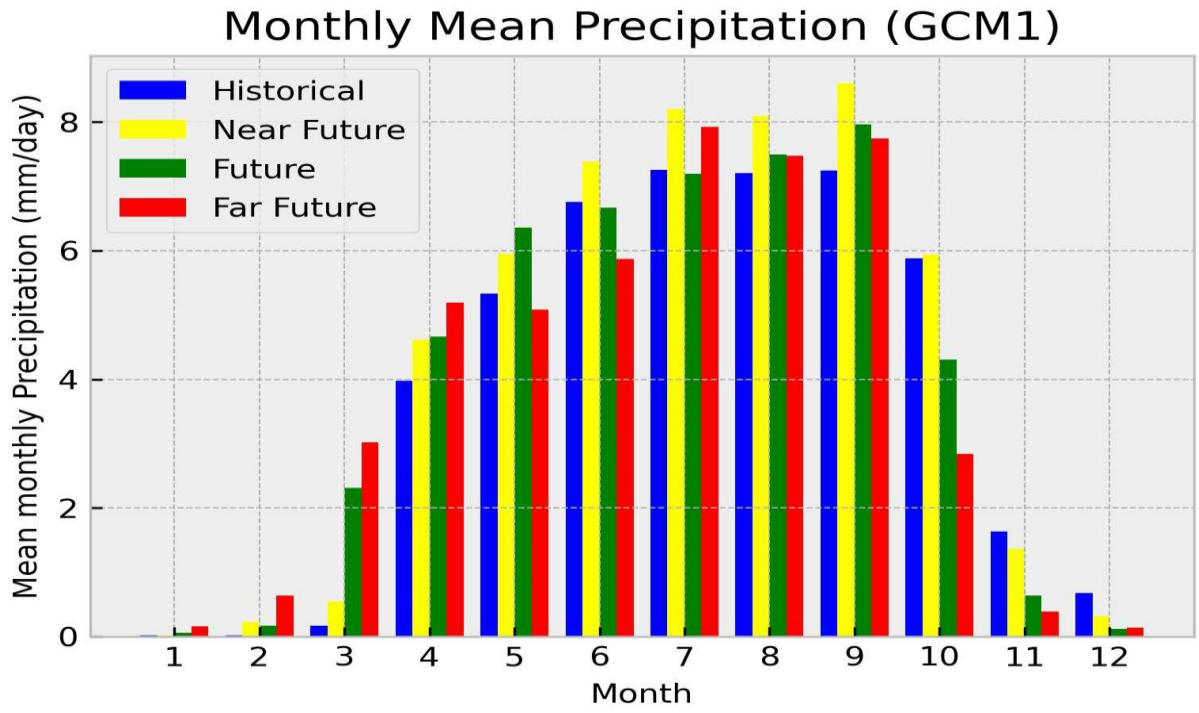

Figure 6 Comparison of the mean monthly precipitation of GCM1 across historical and projected periods (Near future, Future and Far future). Monthly mean precipitation is calculated as the mean of all values falling within each month over a studied period

GCM2 indicates that from January to March the precipitation is increasing from the historical period to the far future period(fig.7). For instance, we see a 5.8mm/day increase from historical period to the far future in March. From October to December, we see a decreasing trend. For example, in October the decrease is highlighted by 2.5mm/day, and it is 15%. From April to September, there is not a specific trend among the months over the period. GCM1 generally predicts smaller changes in precipitation compared to GCM2. For instance, in March, GCM2 predicts a 5.8mm/day increase from the historical period to the far future, while GCM1 predicts a smaller increase of 2.5mm/day. In October, GCM1 projects a more substantial decrease of

about 2.3mm/day (23% decrease) in precipitation compared to GCM2's decrease of 2.5mm/day (15% decrease).

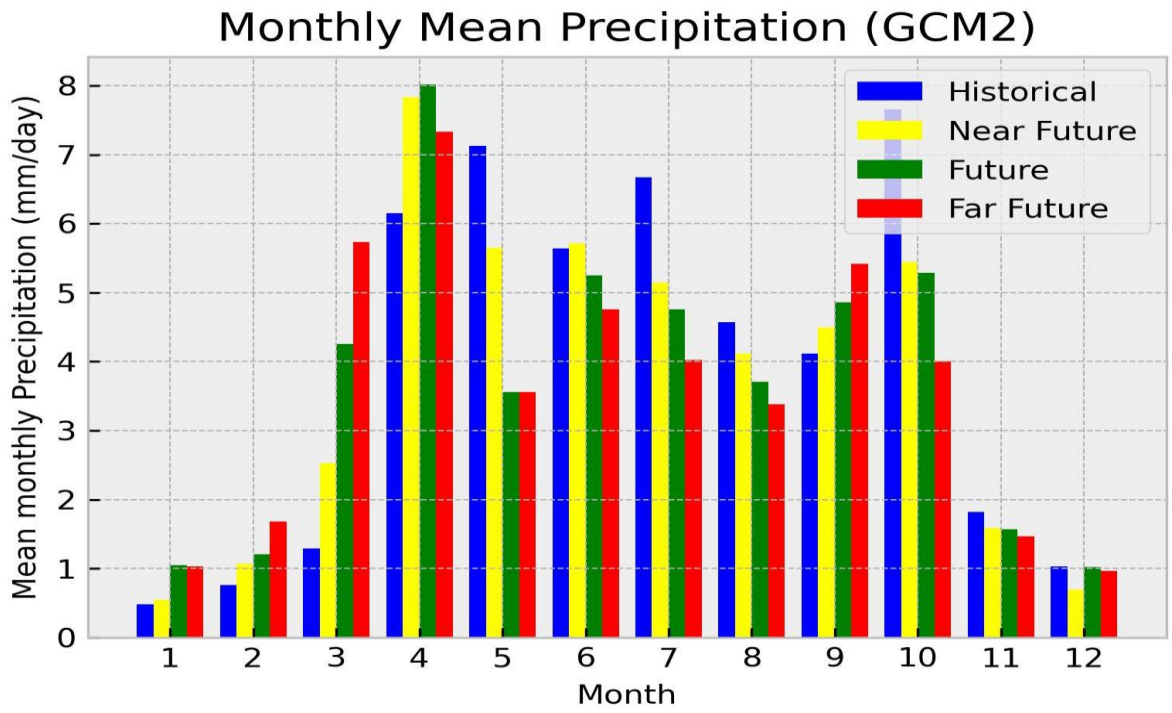

Figure 7 Comparison of the mean monthly precipitation of GCM2 across historical and projected periods (near, Future, and Far future). Monthly mean precipitation is calculated as the mean of all falls within each month over a studied period.

Figure 8 shows that for GCM3 from January to April the precipitation is increasing from the historical period to the far future period. For instance, we see 4mm/day increasing from the historical period to the far future period in April. From October to December, we see a decreasing trend. For example, in October the decrease reaches 3.8mm/day. From May to September there is not a specific trend among the months over the period.

Across the three analyzed Global Climate Models (GCMs), GCM1, GCM2, and GCM3, distinct patterns of monthly precipitation changes emerge from the historical period to the far future period. In GCM1, there is a consistent increase in precipitation from January to April, with March showing a notable 2.5mm/day increase. This contrasts with GCM2, where January to March experiences a more substantial increase in precipitation, with March showcasing a 5.8mm/day rise. Both GCM1 and GCM2 exhibit decreasing trends in precipitation from October to December, albeit with varying magnitudes of decrease. GCM1 indicates a 23% reduction in October, while GCM2 highlights a 15% decrease. From May to September, there

are no specific trends identified across the months for both GCM1 and GCM2. GCM3, on the other hand, follows a similar pattern of increasing precipitation from January to April, with April showing a significant 4mm/day rise. Like the other models, GCM3 also demonstrates a decreasing trend in precipitation from October to December. Throughout the period from May to September, none of the GCMs exhibit distinct trends in precipitation. While all three GCMs indicate consistent increasing trends in precipitation from January to April and decreasing trends from October to December, the magnitude and timing of these changes differ among the models. GCM2 portrays the highest increase in precipitation in both January-March and April, while GCM1 and GCM3 demonstrate relatively lower increases. Furthermore, the variations in the degree of decrease in October and the lack of a specific trend in the mid-year months further underscore the differences in these GCMs' projections for future precipitation patterns.

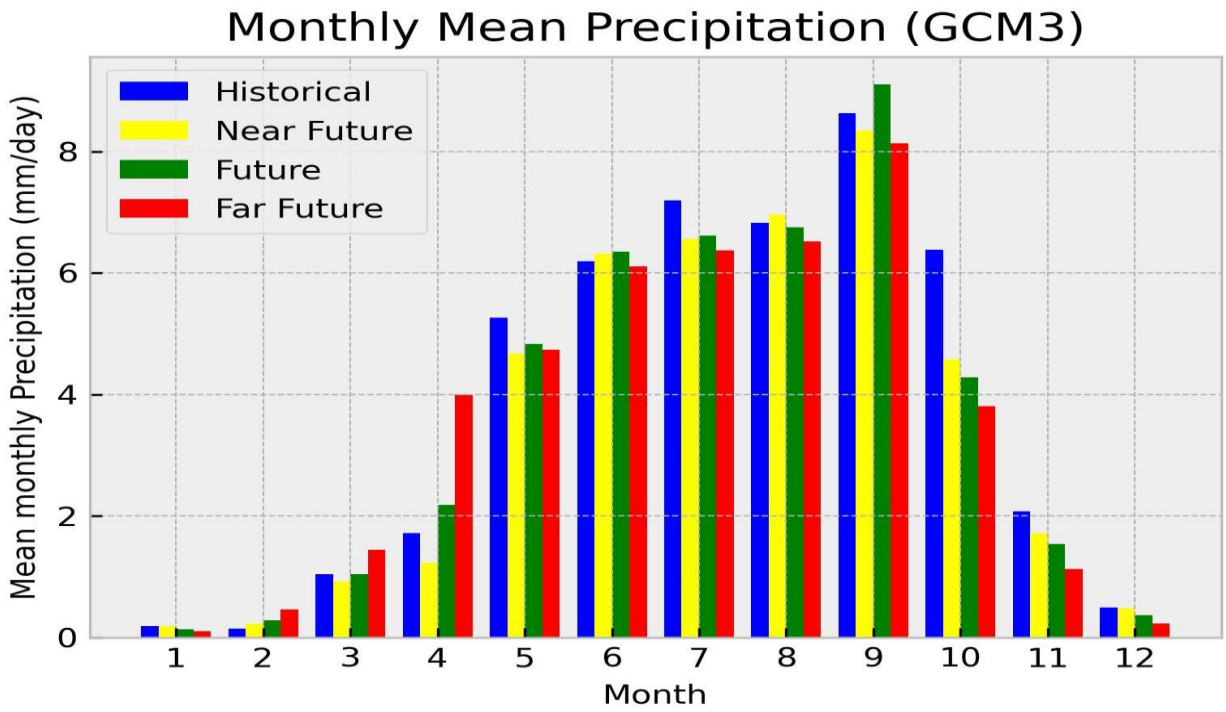

Figure 8 Comparison of the mean monthly precipitation of GCM3 across historical and projected periods (near, Future, and Far future). Monthly mean precipitation is calculated as the mean of all falls within each month over a studied period.

The analysis compares historical data with future projections for monthly precipitation changes using three GCMs, analyzing data for near, future, and far future periods. Monthly Precipitation Change.

The analysis of GCM2, project an interesting pattern where from January to March, there is an increasing trend in precipitation, with March showing a substantial 5.8mm/day increase from the historical period to the far future. This suggests a potential shift toward wetter conditions in these months. Conversely, from October to December, a decreasing trend is observed. October, for example, displays a decrease of 2.5mm/day, which translates to a 15% reduction compared to historical values. The analysis does not find a consistent trend among the months from April to September. GCM1 generally predicts smaller changes in precipitation compared to GCM2. This is evident in the March example, where GCM2 projects a 5.8mm/day increase from historical to far-future periods, while GCM1 predicts a smaller increase of 2.5mm/day. In October, GCM1 projects a more substantial 2.3mm/day decrease (23% decrease) in precipitation compared to GCM2's decrease of 2.5mm/day (15% decrease). These differences highlight the variability between different models in capturing the magnitude of changes. GCM3's projections also show an increasing trend in precipitation from January to April, with April experiencing a 4mm/day increase from historical to far-future periods. Similarly, the October to December period exhibits a decreasing trend, with October seeing a substantial 3.8mm/day reduction. Like GCM2, GCM3 does not display a clear trend from May to September. The analysis then draws comparisons across all three GCMs. It highlights that GCM1, GCM2, and GCM3 each exhibit distinct patterns of precipitation changes. All three models project increasing precipitation from January to April but with variations in the magnitude of change. The same holds true for the decreasing trend from October to December. However, during the months from May to September, none of the models show specific trends. It’s important to note the varying magnitudes of changes predicted by the different GCMs. GCM2, for example, projects the highest increase in precipitation in both January and April, indicating potentially more pronounced changes in these months compared to the other models. These findings have significant implications for understanding how precipitation patterns might evolve in the future. The contrasting trends among the months and the differences between the GCMs underscore the complexity and uncertainty in predicting future climate changes. The analysis allows for a better understanding of the potential timing and magnitude of these changes, which can inform decision-making in sectors like water resource management, and infrastructure planning.

The analysis provides a comprehensive overview of the monthly precipitation changes predicted by different GCMs across multiple time periods. It highlights both consistent trends (increasing precipitation from January to April and decreasing from October to December) and

variations in magnitude and timing. Such insights are valuable for adapting to potential changes in local climate conditions and for making informed decisions in various sectors.

1.3 Annual change in precipitation

Figure 9 shows the variability of annual precipitation of the historical, near future, future, and far future periods. In the figure the historical period has different trends compare to the near future(f1), Future(f2), and far future(f3). Furthermore, delving into the interquartile range (25% - 75%) for each period across the GCMs augments our comprehension of precipitation variability. This range, encapsulating the middle 50% of data distribution, furnishes a comprehensive measure of dispersion. By factoring in the interquartile range, we gain a nuanced understanding of the extent of annual precipitation value spread within each period. The annual precipitation for the historical varies among the different General Circulation Models (GCMs), measuring at 260mm/yr, 450mm/yr, and 200mm/yr respectively. On average, the yearly precipitation is 303mm. Looking ahead from the near future to the distant future, this trend in annual precipitation remains consistent. For instance, in the near future, the annual precipitation is projected to be 230mm/yr, 200mm/yr, and 70mm/yr, respectively with an average of 166mm/yr. In the future scenario, the annual precipitation is anticipated to be 320mm/yr, 170mm/yr, and 50mm/yr. Similarly, the far future exhibits annual precipitation as 170mm/yr, 230mm/yr, and 200mm/yr, averaging at 200mm/yr.

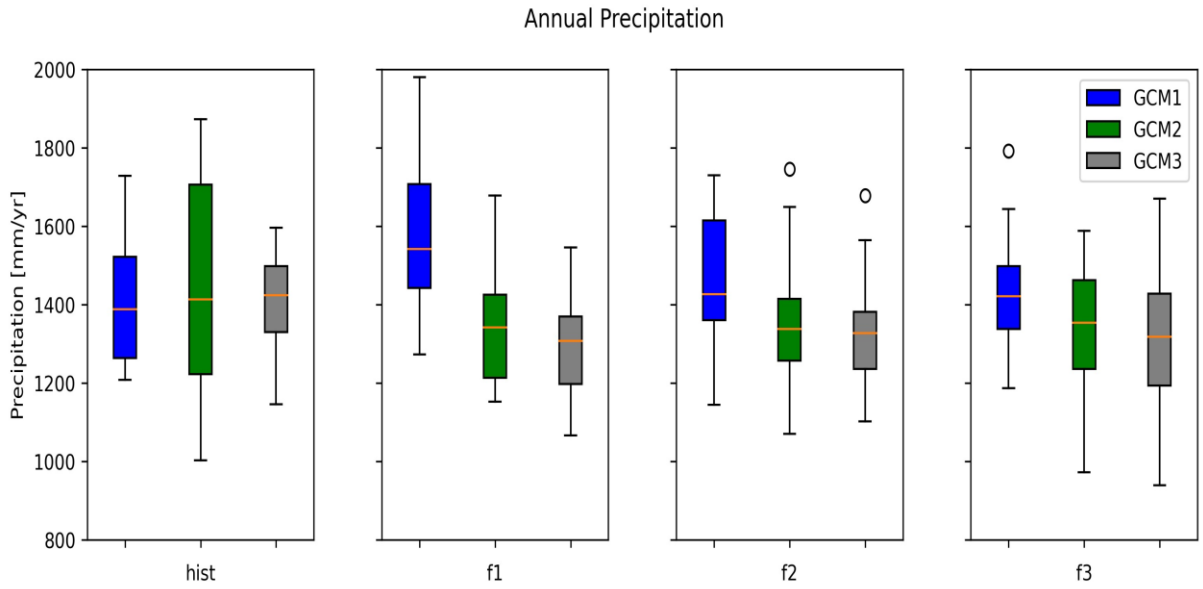

Figure 9 The annual precipitation of the historical and projected periods (near future, Future, and Far future) of each GCM over various scenarios using the historical period (1996-2005 and Projected period 2011-2100). The annual precipitation is calculated as the mean of all values falling within a year

This analysis examines the variability of annual precipitation across different time periods using General Circulation Models (GCMs). It provides insights into how precipitation patterns change over time and how these changes are distributed within each period. The analysis considers the historical period and three future scenarios, revealing different trends in precipitation. The interquartile range (IQR) is introduced to measure dispersion for each period across different GCMs, providing a more comprehensive understanding of the variability in annual precipitation. The analysis reveals that annual precipitation values vary among different GCMs for the historical period, with measurements of 260mm/yr, 450mm/yr, and 200mm/yr. The average annual precipitation across the GCMs for the historical period is 303mm/yr, highlighting the diversity in model projections. The analysis discusses how the trend in annual precipitation remains consistent as we move from the near future to the far future. For example, in the near future scenario, the annual precipitation is projected to be 230mm/yr, 200mm/yr, and 70mm/yr, averaging at 166mm/yr. The same approach is applied to the future and far-future scenarios, with corresponding values presented. The analysis emphasizes averaging annual precipitation values across different GCMs for each period, providing a more robust representation of potential future climate conditions, considering the uncertainties associated with individual models. The results provide insights into how the distribution of annual precipitation values might change over time, which is crucial for understanding potential changes in streamflow and potential hydropower generation.

In conclusion, this analysis underscores the importance of considering the variability and consistency of annual precipitation patterns across different time periods using GCMs. By examining historical, near future, future, and far future scenarios, the study provides valuable insights into the potential changes in precipitation distribution over time. The approach of averaging across GCMs enhances the reliability of projections and assists in preparing for a range of possible climate outcomes. This research contributes to the broader understanding of climate change impacts and helps guide strategies to mitigate and adapt to changing precipitation patterns.

1.4 Change in Temperature

The result of this section presents the changes in temperature by analyzing the long-term average temperature, monthly mean temperature of the catchment. Three Global models (GCMs) were selected to assess the changes in Temperature. These models were chosen to capture a wide range of expected climate uncertainties. The findings are summarized in Figures 10,11,12,13. The findings were presented by plotting various graphs to indicate the increase or decrease in temperature.

Figure 10 shows that the three future periods have higher temperatures than that of the historical period. The three GCMs shows an increasing trend from the historical period to the three future periods. GCM1 shows there is an increase trend from 21℃ to 26℃, GCM2 19℃ to 24℃ and GCM 3 18℃ to 22℃.GCM1 we see a higher temperature in the far future than the historical. Generally, the three GCMs of (fig.10) have an average of 19.3℃ in the historical period, and 21.2℃,22.23℃, and 24℃ in the three future periods. The changes from historical to near future, future and far future in temperature are 9.8%,15%, and 24% respectively.

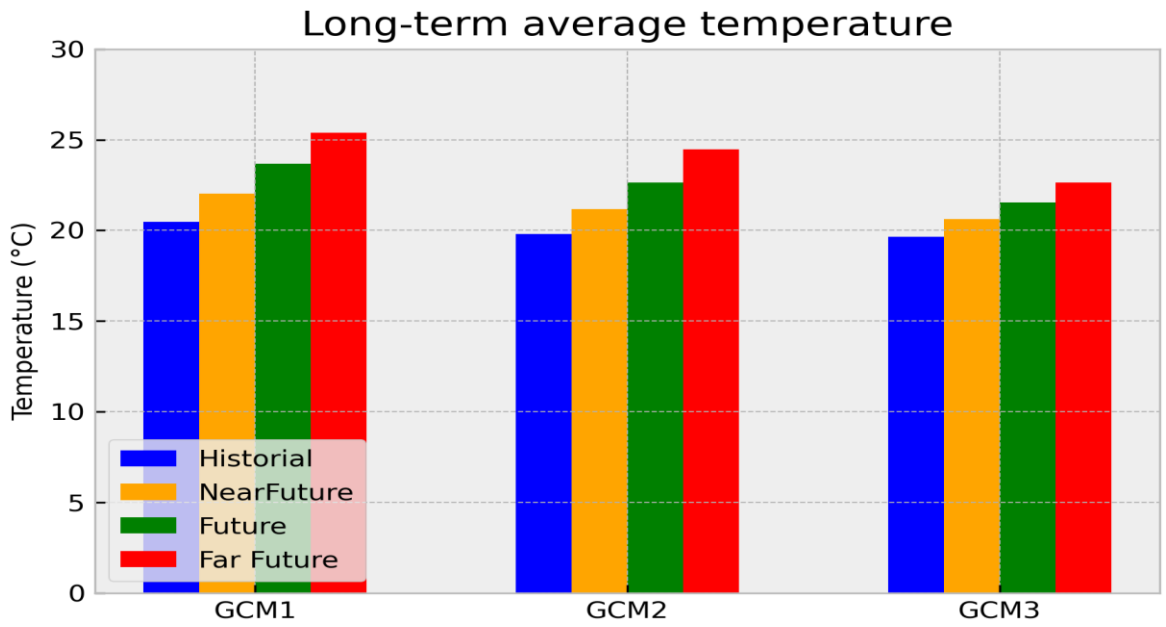

Figure 10 represents the changes in temperature over the historical and projected periods, considering the near future, future, and far future. The long-term average temperature is calculated as the Sum of all temperatures divided by the Number of days 365.25.

Table 3: average values of the long- term average temperature of the three GCMs in each time periods

	Long-term average Temperature(◦C)			
Periods	GCM1	GCM2	GCM3	Average
Historical period	21℃	19℃	18℃	19℃
Near future period	22℃	21℃	20.6℃	21℃
Future period	23.7℃	22℃	21℃	22℃
Far future period	26℃	24℃	22℃	24℃s

The analysis of temperature trends, as depicted in Figure 10, constitutes a critical element of this study's investigation into climate change impacts. Figure 10 clearly illustrates that all three General Circulation Models (GCMs) project an upward increase in temperatures across historical and future periods, signifying a substantial warming trend. Notably, GCM1 predicts the most significant increase, with temperatures rising from 21°C in the historical period to

26°C in the far future. GCM2 and GCM3 also forecast notable increases, with respective temperature increments from 19°C to 24°C and from 18°C to 22°C. The averaged temperatures across the three GCMs reveal a clear pattern of warming, with the historical period averaging 19.3°C, while the near future, future, and far future periods project averages of 21.2°C, 22.23°C, and 24°C, respectively. These findings underscore the urgency of addressing climate change, as the percentage changes from historical to near future 9.8%, future 15%, and far future 24% indicate a substantial and accelerating warming trend. This temperature analysis not only contributes to the broader understanding of climate change but also underscores the relevance of this research to address the potential consequences of rising temperatures on our environment, ecosystems, and societies.

The analysis in Figure 10 provides a comprehensive understanding of temperature shifts using GCMs across various time periods. It illustrates the rising temperatures in the future compared to historical levels, highlights model variability through GCM1's unique trend, and emphasizes the importance of considering average values across models. The quantification of temperature changes and the subsequent discussion of precipitation trends contribute to a holistic assessment of climate impacts, aiding in informed decision-making and adaptation strategies to improve the pattern of streamflow and hydropower potential in Africa.

1.5 Monthly mean Temperature

Figure 11 shows the monthly mean temperature of the historical to the three future periods GCM1. The figure indicates an increase in temperature from January to February there of the historical period to the far future periods. For instance, we see an increase from 22℃ to 28℃ which is 6℃ increases from the historical period to the far future in February. From January to December, we see an increasing trends of temperature for every month trend.

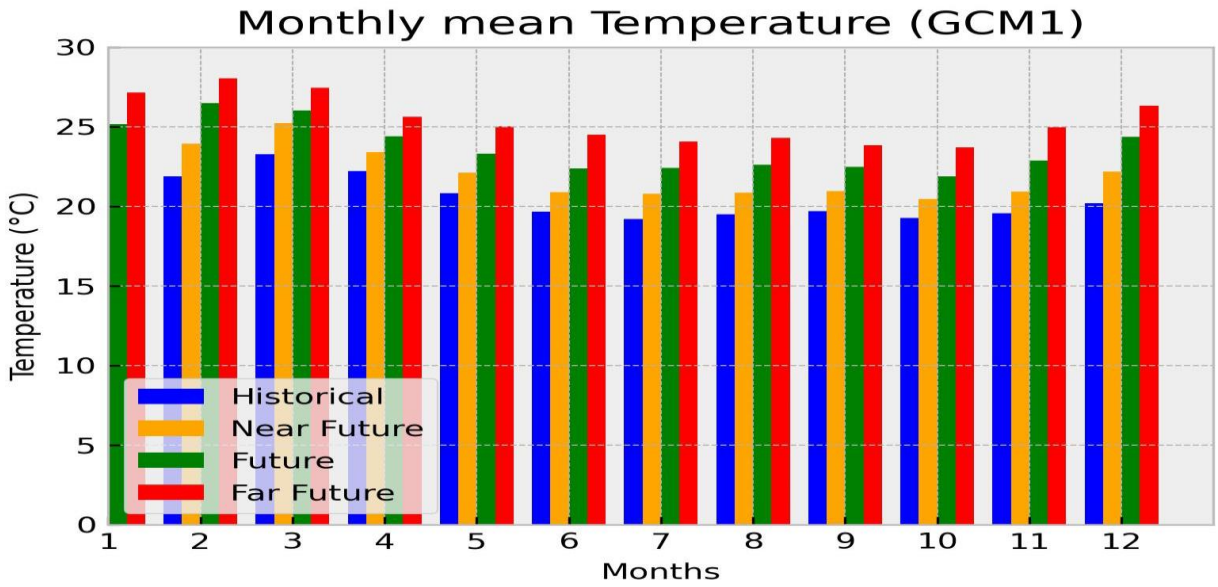

Figure 11 Comparison of the monthly mean temperatures of the various scenarios, the historical period, and the projected period across 12 mean monthly values. The monthly mean temperature is calculated as the sum of daily averages divided by the number of days.

Figure 12 shows the mean monthly temperature of the historical to the three future periods. The figure indicates an increase in temperature from January to December of the historical period to the far future period across all period. For instance, we see from 22℃ to 27℃ increase in February of the historical period to the far future. January also shows the different trends of the missing historical and near future, this is due the performance of the models.

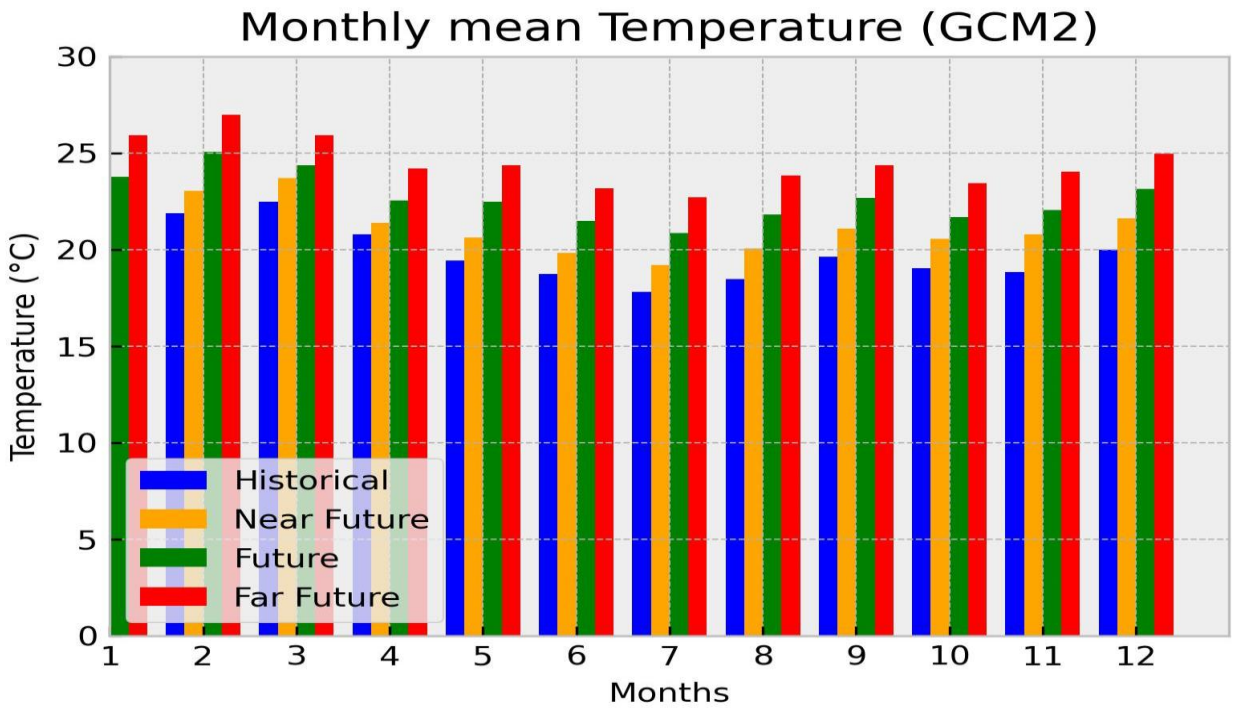

Figure 12 Comparison of the monthly mean temperatures of the various scenarios, the historical period, and the projected period across 12 mean monthly values. The monthly mean temperature is calculated as the sum of daily averages divided by the number.

Figure 13 shows the mean monthly temperature of the historical to the three future periods. The figure indicates an increase in temperature from January to December of the historical to the far future across all periods. For instance, we see about 22℃ to 26℃ increases from the historical period to the far future in February. There is 4℃ increases in the month of February. From April to December, we see similar trend of increase in temperature in December. For example, in December we also see 20℃ to 23℃ increases. January also shows the different trend of the missing historical and near future, this is due to the performance of the models.

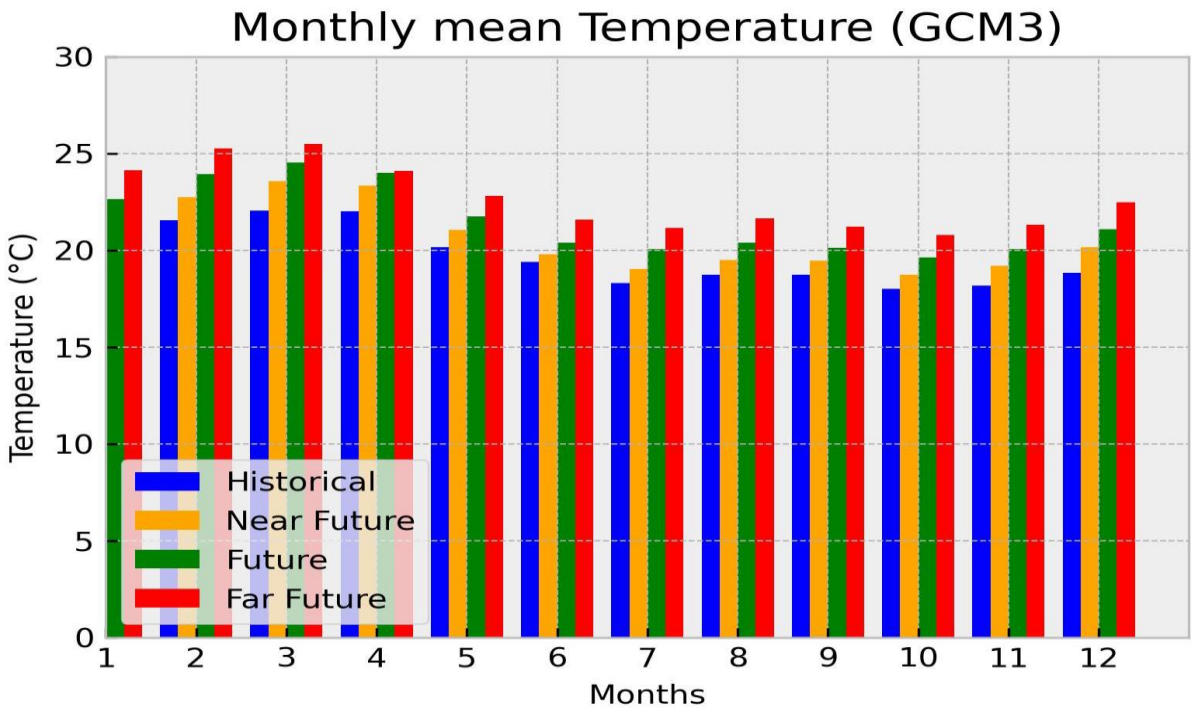

Figure 13 Comparison of the monthly mean temperatures of the various scenarios, the historical period, and the projected period across 12 mean monthly values. The monthly mean temperature is calculated as the sum of daily averages divided by the number.

The analysis presented in Figures 11, 12, and 13 provides a detailed examination of the changing patterns of monthly mean temperatures across historical and future periods using GCM1. These figures offer valuable insights into the temporal evolution of temperatures, shedding light on the trends and variations that shape our understanding of climate change.

In Figure 11, the focus is on the monthly mean temperature trends from historical to far future periods using GCM1. The data underscores a consistent upward shift in temperatures for each month, from January to December, across all periods. This systematic increase reflects the broader global warming trend associated with climate change. Specifically, for example the monthly temperature is presented for February, showcasing a significant 6°C increase from 22°C in the historical period to 28°C in the far future. This noteworthy increase underscores the magnitude of potential temperature changes in shorter time frames, potentially leading to various environmental impacts. However, Figure 12 offers a broader perspective by showing the mean monthly temperature trends from January to December across historical and future periods using GCM1. The data highlights an overall warming trend across all months, where temperatures increase from the historical period to the far future. For instance, February showcases an increase from 22°C to 27°C, underlining the consistent warming trend. Notably,

variations between historical and near future temperatures in January can be attributed to model performance differences, an important aspect to consider when interpreting and utilizing climate model outputs. Moving on to Figure 13, which also illustrates mean monthly temperature trends across historical and future periods using GCM1, the patterns remain consistent. The temperature increase is observed from January to December for all periods. For example, February experiences a rise from about 22℃ to 26℃ in the far future, translating to a 4℃ increase. Similarly, a consistent trend is noted from April to December, with December showcasing a 20℃ to 23℃ increase. The recurring theme of rising temperatures emphasizes the long-term implications of climate change on streamflow pattern and hydropower potential in Africa.

Overall, these analyses offer crucial insights into the intricate and evolving patterns of temperature changes over time. The consistent warming trends across all three figures underscore the pressing need for robust climate mitigation and adaptation strategies. It is important to recognize the inherent complexities of climate modeling, as variations between historical and near-future data points emphasize model performance differences. These insights contribute significantly to the body of knowledge addressing the impacts of climate change and provide a foundation for informed decision-making in policies and practices in the African region.

3. Streamflow change under changing climate

This section focuses on analyzing the changes in streamflow (Q) at long-term average daily streamflow for each ensemble (looking at uncertainty in ensembles) annual mean streamflow, (mean of streamflow simulations of all ensembles within a specific year indicating interannual variability) Seasonal pattern of streamflow between historical and projected period in the catchment.

3.1 Time series of streamflow

Figure 14 shows the streamflow simulations using GCM1 over the entire time period. The figure provides insight into the streamflow trend from 2030 to 2100. For instance, the time series analysis reveals a notable pattern in the streamflow data during this extended period. But we see, the observed time series showcases a consistent decreasing trend in streamflow, fluctuating from an initial value of 440 m3/s down to 250 m3/s. This observed trend over the specified time range signifies a reduction in streamflow for GCM 1.

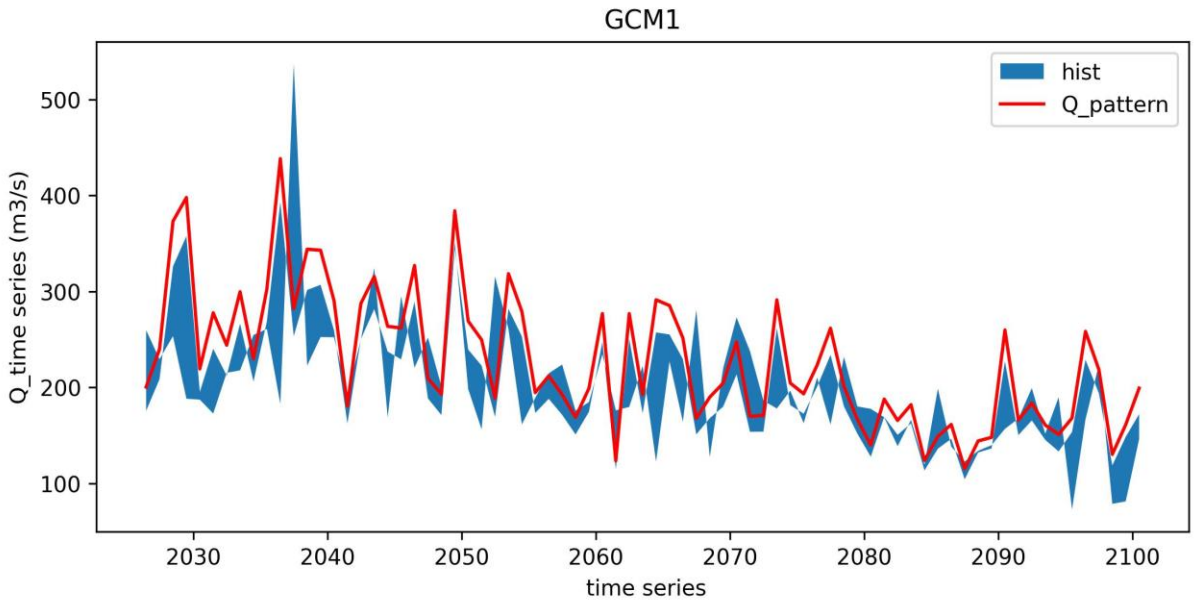

Figure 14: GCM 1 show the time series pattern of streamflow from 2025-2100

Figure15 shows streamflow simulations using GCM2 across all the period. we see a streamflow trend around 2030-2100. Generally, the time series shows the decreasing trend of streamflow, for example, the maximum peak flow change from 500m^3/s to 200m^3/s from historical period to the far future. The time series also shows the uncertainty of GCM2 pattern of streamflow trend for GCM 2.

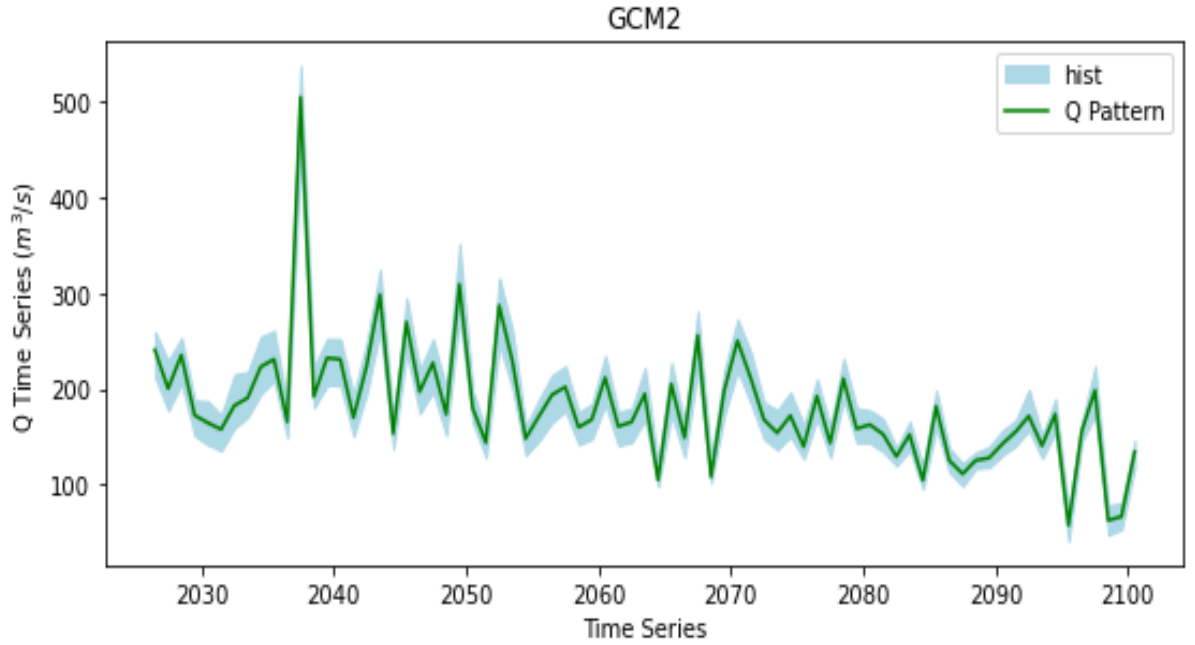

Figure 15: shows the time series pattern of streamflow from 2025-2100

Figure16 shows streamflow simulations using GCM3 across all the period. we see a streamflow trend around 2030-2100. Generally, the time series shows the decreasing trend of streamflow from 300m3/s to 200m3/s similar to GCM2. The time series also shows the uncertainty of GCM3 pattern of streamflow trend for GCM 3.

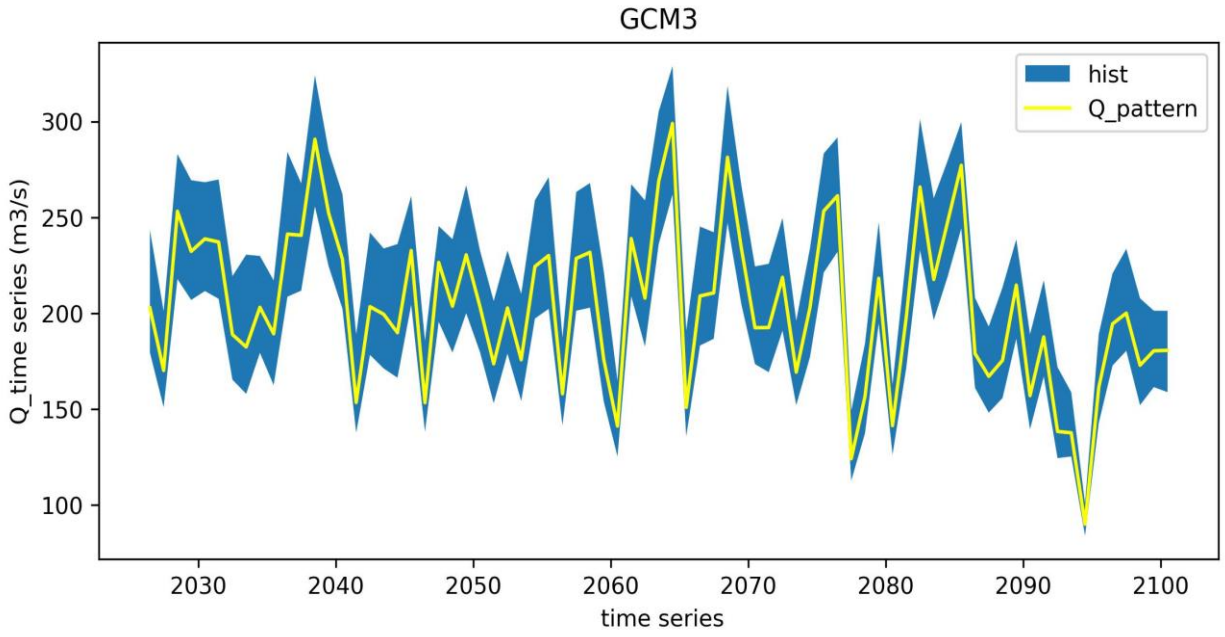

Figure 16:Time series pattern of streamflow from 2025-2100.

The analysis presented in Figures 14, 15, and 16 offers a comprehensive assessment of streamflow simulations over extended time periods, using three different General Circulation Models (GCMs). These figures provide valuable insights into the anticipated streamflow trends, enabling a deeper understanding of potential impacts on water resources and ecosystems.

Figure 14 provides the insightful depiction of streamflow simulations using GCM1 over the timeframe from 2030 to 2100. The time series analysis offers a revealing pattern in the streamflow data throughout this extended period. A notable observation is the consistent decreasing trend in streamflow values. The fluctuations, starting at 440 m^3/s and declining to 250 m^3/s, signify a pronounced reduction in streamflow for GCM1. This pattern suggests potential challenges for Streamflow pattern and hydropower potential. The streamflow simulations using GCM2 across the entire time period of figure 15 shows that time series data underscores a recurring theme of decreasing streamflow. The maximum peak flow demonstrates a substantial change, plummeting from 500 m^3/s in the historical period to 200 m^3/s in the far future. Additionally, the time series reveals the inherent uncertainty in GCM2's

pattern of streamflow trend. Similarly, Figure 16 captures the streamflow simulations using GCM3 across the analyzed period. A decreasing streamflow trend emerges from this time series analysis as well. The peak flow values mirror those of GCM2, declining from 500 m^3/s to 200 m^3/s. This parallel decrease between GCM2 and GCM3 underscores the consistency in their projections. Again, the time series emphasizes the uncertainty embedded in GCM3's pattern of streamflow trend. Collectively, these analyses offer significant insights into potential streamflow changes. The consistent downward trend in streamflow across all three GCMs from historical to future periods suggests an impending challenge. Reduced streamflow can lead to low runoff, affecting the pattern of streamflow and hydropower potential. The convergence of decreasing trends between GCM2 and GCM3 further reinforces the notion of a changing hydrological landscape. The inherent uncertainty highlighted by the varying patterns of streamflow trends within each GCM underscores the need for cautious interpretation.

The presented analysis in Figures 14, 15, and 16 contributes significantly to our understanding of streamflow trends and their potential implications. These findings provide valuable insights on streamflow pattern over time. The discussion of model uncertainty underscores the dynamic nature of climate modeling and the importance of a multi-faceted approach to address the challenges posed by changing streamflow patterns.

3.2 Long-term average daily streamflow

Figure 17 shows that the three future periods generally have a decreasing trend of long-term average daily streamflow compared to the historical period. However, GCM1 shows an increase in long-term average daily streamflow in the near future period. Generally, GCM 1 shows a change in the long-term average daily streamflow of the future periods of 75m^3/s from the historical period to far future period, which suggests streamflow may decrease 30% in the far future period. GCM2 and GCM3 show decreasing changes in the long-average daily streamflow from the historical period to the future period about 100 m^3/s and 60m^3/s, respectively, which corresponds to the decrease of 40% and 25% of the historical streamflow. The general change of long-term average streamflow of the three future periods is a decrease of 78m^3/s and the relative decrease is 30%.

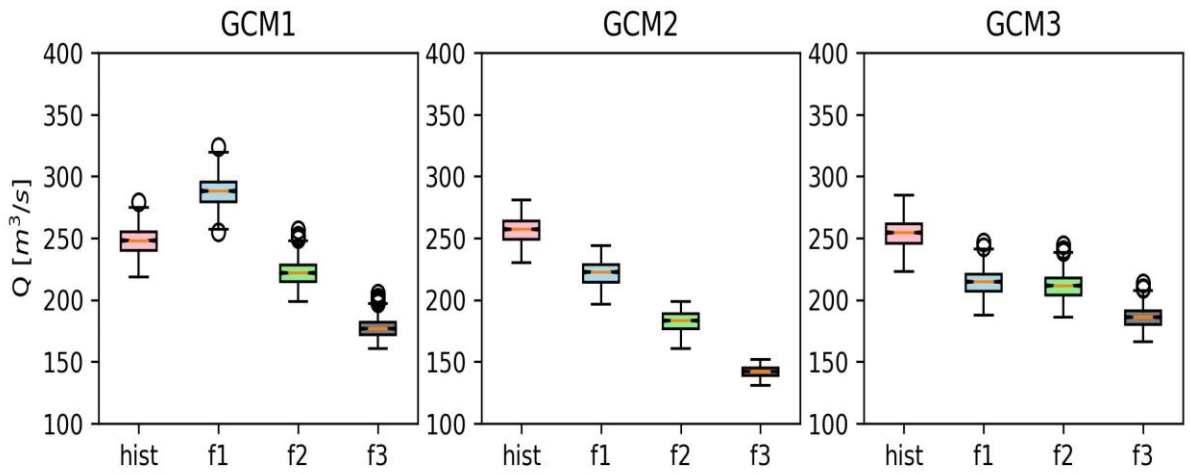

Figure 17: Variability in daily streamflow across different time periods using three GCMs. We calculated the average of streamflow over each period and the box shows the variability of 738 ensembles.

The analysis presented in Figure 17 regarding the long-term average daily streamflow and the projections for different future periods offers valuable insights into the potential trends and changes in streamflow. This analysis highlights the impact of climate change on streamflow patterns, which has significant implications on streamflow patterns and hydropower generation in Africa. The observed trends in the long-term average daily streamflow indicate a general decrease in streamflow for future periods compared to the historical period. This decreasing trend raises concerns about the streamflow pattern in the study area. However, GCM1 presents an interesting outlier, showing an increase in streamflow during the near future period. This discrepancy emphasizes the uncertainties and variations inherent in climate models and projections. GCM1's projection of increased streamflow in the near future period could be due to various factors such as local climate patterns, changes in precipitation regimes, or specific characteristics of the study area. This divergence underscores the complexity of predicting future streamflow. It would be valuable to investigate the reasons behind this anomaly, as it might provide insights into factors that can influence streamflow dynamics. When examining the changes in streamflow across the different GCMs, GCM2 and GCM3 show consistent decreasing trends in long-term average daily streamflow, with projected changes of 100 m^3/s and 60 m^3/s, respectively, relative to the historical period. These changes correspond to decreases of 40% and 25% of the historical streamflow, respectively. These considerable reductions highlight the potential challenges that water resource managers and policymakers may face in the future, necessitating adaptive strategies to ensure sustainable water use and management. The combined analysis of all three GCMs indicates a general decrease in the long-

term average streamflow across the three future periods, with an average change of 78 m^3/s and a relative decrease of 30% compared to the historical period. This collective trend underlines the urgency of addressing climate change and its implications for water resources. The observed decrease in streamflow has multifaceted consequences, including impacts on streamflow pattern and hydropower generation

In conclusion, the analysis presented a comprehensive understanding of the potential changes in long-term average daily streamflow due to climate change. The varying projections from different GCMs, particularly the outlier scenario of GCM1, emphasize the need for a nuanced interpretation of climate models and an awareness of their uncertainties. The overall decreasing trend in streamflow across future periods underscores the importance of proactive measures to mitigate and adapt to the impacts of climate change on water resources.

3.3 Annual streamflow

Figure 18 provides insight into the trends of annual streamflow across different time periods. Notably, the analysis demonstrates that all three future periods exhibit a declining trend in annual streamflow when compared to the historical period. However, GCM1 showcases a distinct pattern by exhibiting an increase in annual streamflow during the near future, contrasting with GCM2 and GCM3.Specifically, GCM1 presents an increase in annual streamflow during the near future period, setting it apart from the other two GCMs. Meanwhile, GCM2 and GCM3 both show a decrease in annual streamflow across the three future periods, consistent with the overarching trend. In terms of specifics, GCM1 indicates a change of 60 m3/s of the interquartile range in annual streamflow during the future periods. GCM2 and GCM3, on the other hand, display changes in annual streamflow of 43 m3/s and 46 m3/s respectively during the three future periods. The cumulative analysis of the three GCMs reveals a general change in annual streamflow of 49.6 m3/s across the three future periods.

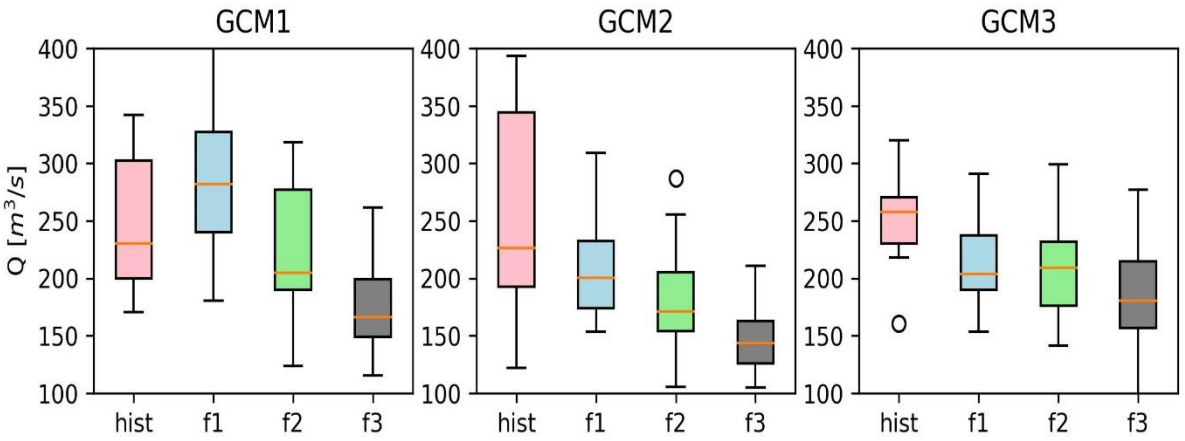

Figure 18: Box plot comparing streamflow data for various years across the historical period (1996-2005) and projected period (2011-2100) using three Global Climate Models (GCMs). Annual streamflow here is the mean of streamflow of all ensembles over a year This aims is to show the temporal variability of annual streamflow.

The analysis presented in Figure 18 regarding the trends in annual streamflow and the implications of these findings in the context of the impacts of climate change on streamflow for potential hydropower generation in Africa

The analysis of annual streamflow trends across different time periods, as depicted in Figure 18, provides valuable insights into the potential impacts of climate change on streamflow pattern. It is evident that all three GCMs project a decline in annual streamflow for the future periods when compared to the historical period. This consistency in projected decrease underlines the importance of understanding and addressing the potential consequences of altered hydrological patterns due to changing climate conditions.

The analysis of annual streamflow trends across different time periods, as depicted in Figure 18, provides valuable insights into the potential impacts of climate change on water resources. It is evident that all three GCMs project a decline in annual streamflow for future periods when compared to the historical period. This consistency in projected decrease underlines the importance of understanding and addressing the potential consequences of altered streamflow patterns due to changing climate conditions. An interesting observation arises from GCM1, which exhibits a distinct pattern by projecting an increase in annual streamflow during the near future period. This deviation from the declining trend seen in GCM2 and GCM3 emphasizes the inherent variability and uncertainties associated with climate models. The divergence among the GCMs, particularly the anomaly presented by GCM1, underscores the need for cautious interpretation of individual model outputs and highlights the complexity of predicting

future streamflow patterns. The projected declining trends in annual streamflow, evident across all GCMs except for GCM1, have significant implications for water resource management strategies. The anticipated decrease in streamflow can pose challenges in many ways such as low runoff which may lead to low streamflow patterns that may affect the generation of hydropower. Adaptation measures such as water conservation, efficient irrigation practices, and the development of resilient water management plans are crucial to mitigate the potential impacts of reduced streamflow. The unique projection from GCM1, indicating an increase in annual streamflow during the near future period, could be attributed to various local factors, such as specific topographical characteristics or regional climate influences. This underscores the importance of considering local conditions when interpreting model outputs and making informed decisions based on projections. Additionally, it's important to acknowledge the limitations of climate models in capturing all relevant factors that can influence streamflow patterns. The cumulative analysis of the three GCMs reveals an average change of 49.6 m^3/s in annual streamflow across the three future periods. This overarching trend of decreasing streamflow emphasizes the urgency of integrating climate change considerations into water resource policies and planning efforts.

The trends in annual streamflow projections as analysed in Figure 18 underscore the complex interplay between climate change, hydrological patterns, and water resource management. The varying outputs from different GCMs and the presence of an outlier scenario emphasize the importance of considering multiple perspectives when planning for the potential impacts of changing streamflow patterns. Decision-makers should be prepared to implement adaptive strategies that address potential water scarcity, manage competing water demands, and ensure the sustainability of water resources in the face of changing hydrological conditions.

3.4 Seasonal Pattern of Streamflow

Figure 19 illustrates the trends in the seasonal pattern of streamflow for GCM1. The analysis reveals a consistent pattern from January to April, with minimal change observed between the historical and future periods. However, a notable increase in streamflow becomes evident in the near future period, spanning from May to November, showcasing a more substantial surge in the seasonal streamflow pattern. Notably, the figure depicts a peak flow of 700 m3/s during the near future period, specifically from June to December. The associated trend exhibits a consistent increase in streamflow over this time frame, with the uncertainty the peak flow can reach 780 m3/s. In contrast, during the historical period, the streamflow reaches its maximum

seasonal pattern of 490 m3/s, occurring from October to December. This pattern is characterized by a certain level of uncertainty, measuring 600 m3/s.

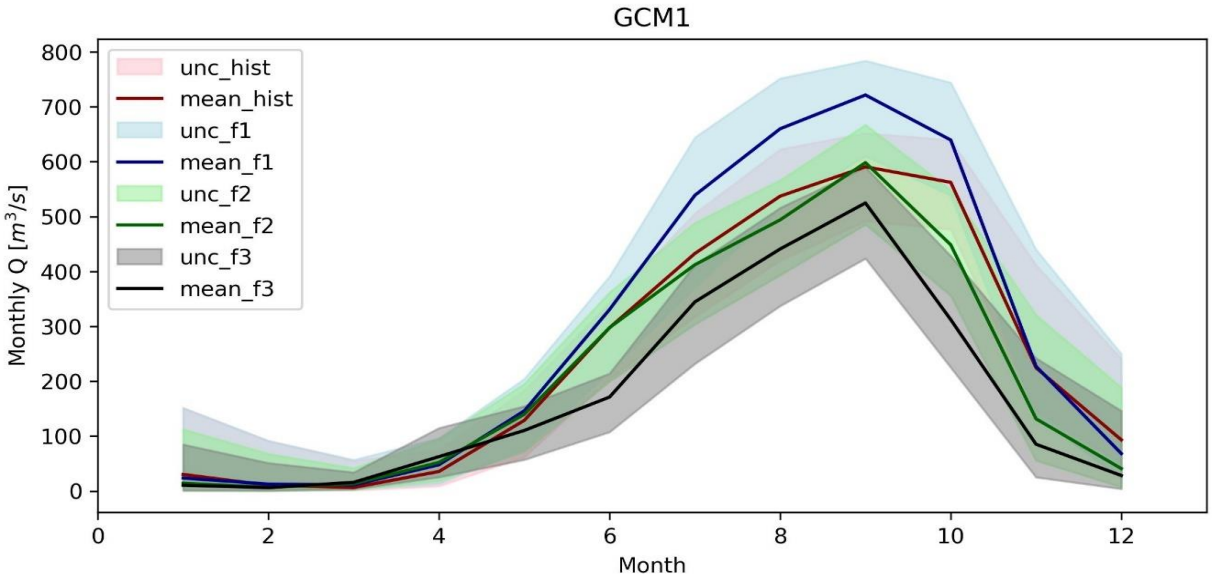

Figure 19: GCM1Estimated change in the mean monthly streamflow pattern over 12 months. The seasonal streamflow is calculated as the average streamflow for the months divided by the overall mean and multiplied by 100.

Figure 20 shows the trends in the seasonal pattern of streamflow for GCM2. The analysis indicates that there is minimal change observed from January to May when comparing the historical period to the future periods. However, a distinct shift is evident from June to December, where both historical and future periods exhibit varying trends in seasonal streamflow along with associated uncertainties. During the historical period, the maximum flow of streamflow occurs in October to December, reaching a value of 500 m3/s. This increase in flow is accompanied by a maximum uncertainty of 600 m3/s. Conversely, a decrease trend is noted for the near future period, with a drop of 300 m3/s in September. The uncertainty associated with this decrease is 400 m3/s. The recurring theme of a decrease trend is further confirmed by the observation that the historical period's trend continues in the near future. The trends suggest a decrease in streamflow from October to December, which is a recurring feature across historical, near future, future, and far future periods.

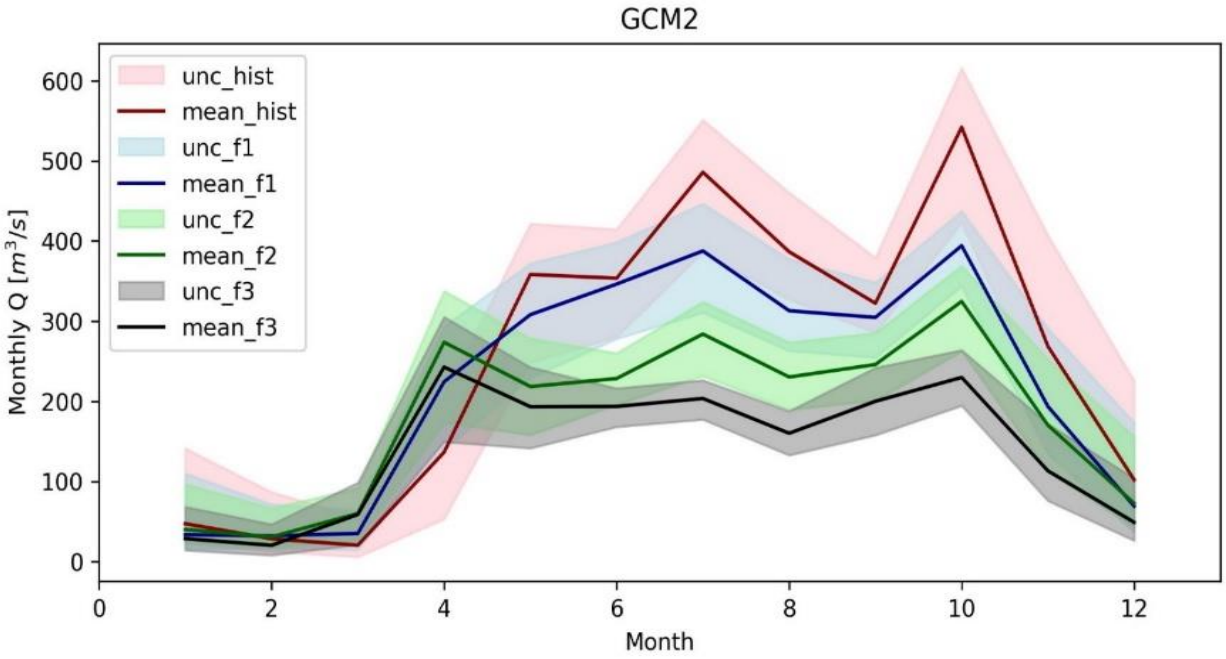

Figure 20: GCM2 Estimated change in the mean monthly streamflow pattern over 12 months. The seasonal streamflow is calculated as the average streamflow for the months divided by the overall mean and multiplied by 100.

over the historical and projection period from January to December of the various scenarios, historical, near future, future, and far future. The observation of GCM2 shows limited changes in the streamflow pattern from January to March and an increase in streamflow across the four scenarios compared to GCM1 and GCM3 from April to December with a lower uncertainty of from April to August 400m^3/s and a higher uncertainty from September to November 600m^3/s.

Figure 21shows the trends in different months of seasonal pattern of streamflow GCM3 The figure shows no change from January to April from the historical period to the future periods. But we see an increase and decrease trend of the historical and future periods of seasonal streamflow its uncertainty from May to December. For instance, the figure shows maximum trend of streamflow of the historical period 620m^3/s increase with a maximum uncertainty of 700m^3/s. Generally, the three future periods show a seasonal pattern of streamflow of 600 m^3/s from July to December, with an uncertainty of 600m^3/s,625 m^3/s with an uncertainty of 800 m^3/s, and 500 m^3/s with the uncertainty of 550 m^3/s respectively.

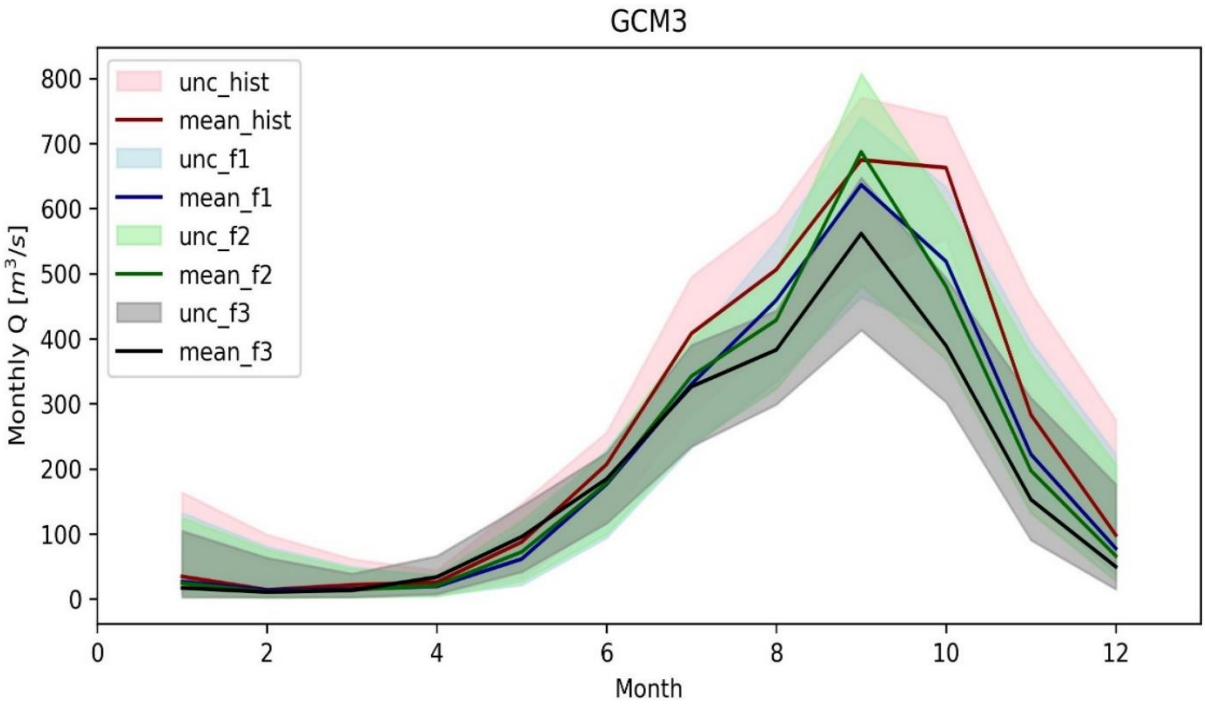

Figure 21: GCM3 Estimated change in the mean monthly streamflow pattern over 12 months. The seasonal streamflow is calculated as the average streamflow for the months divided by the overall mean and multiplied by 100.

The analysis depicted in Figures 19, 20, and 21 offers a comprehensive understanding of the projected changes in the seasonal pattern of streamflow across different GCMs. These figures highlight both consistencies and discrepancies in the projected trends, emphasizing the complex nature of climate change impacts on streamflow.

Figure 19 provides insights into the seasonal pattern of streamflow as projected by GCM1. The observed minimal change in streamflow from January to April between historical and future periods suggests a relatively stable hydrological regime during this time frame. However, the noteworthy increase in streamflow from May to November, particularly during the near future period, points to a significant alteration in the streamflow dynamics. This substantial surge is illustrated by a peak flow of 700 m^3/s during the near future period, The associated uncertainty, ranging up to 780 m^3/s, highlights the challenges of precisely predicting the magnitude of this change. Figure 20 provides insights into the seasonal pattern of streamflow as projected by GCM1. The observed minimal change in streamflow from January to March between historical and future periods suggests a relatively stable hydrological regime during this time frame. However, the noteworthy increase in streamflow from April to December, particularly during the near future period, points to a significant alteration in the streamflow dynamics. This

substantial surge is illustrated by a peak flow of 550 m^3/s during the near future period, The associated uncertainty, ranging up to 600 m^3/s, highlights the challenges of precisely predicting the magnitude of this change. Figure 21 presents a unique perspective on the seasonal pattern of streamflow as projected by GCM3. The analysis reveals minimal change from January to April across historical and future periods. However, from May to December, there is a combination of both increase and decrease trends, along with associated uncertainties. The most notable finding is the projection of a maximum historical streamflow trend of 620 m^3/s, which contrasts with the future periods' more consistent trends. The projected seasonal streamflow patterns for the three future periods, ranging from 500 m^3/s to 625 m^3/s, underscore the uncertainties in predicting exact streamflow values but emphasize the persistence of these trends.

However, the finding of this study has significant implications for understanding the potential effects of changing climate patterns on streamflow and hydropower generation in Africa, Genale Dawa III (GD-3) in Ethiopia. A comparative analysis across GCMs reveals intriguing variations in streamflow patterns. While all three GCMs project decreasing trends in streamflow, GCM1 exhibits a unique characteristic. In the near future period, GCM1 shows an increase in streamflow, in contrast to the decreasing trends in GCM2 and GCM3. This distinctive behavior observed in GCM1 aligns with previous research (Zheng et al., 2009), emphasizing the role of temperature and precipitation in influencing streamflow trends. Through the analysis of historical streamflow data and climate data, several observations have emerged, shedding light on the challenges and opportunities facing on the region’s energy sector. The analysis of historical streamflow data revealed decrease change in seasonal patterns across the time period (historical and projection periods). A clear trend of decrease in streamflow of the near future, future and far future was evident, while others experienced a more unpredictable streamflow behavior due to high temperature and low precipitation. These findings align with Zheng et al. (2009) which highlights the role of precipitation and temperature in influencing streamflow patterns. They indicated that the reduction of precipitation accounts for a significant portion of the observed decrease in streamflow. Similarly, (Kankam-Yeboah et al., 2013) indicated that the increase in temperature can further exacerbate the reduction in streamflow. The analysis of streamflow patterns across various GCMs presents a consistent narrative of decreasing trends in streamflow over the specified time periods. The divergence in behavior observed in GCM1 underscores the complexity of climate-

driven streamflow change. The finding from the research indicates a 30% general change in long-term average, and an annual change of 42.2% of streamflow reduction in the future.

4. Change in hydropower generation in the future

The change in hydropower generation of the Genale Dawa III (GD-3) in Ethiopia can be assessed by comparing the hydropower potential between different period, such as the historical period (1996-2005) and the future periods (2011-2100). This analysis helps to understand how climate change may affect the availability of hydropower potential.

4.1 Time Series of Hydropower Potential

Figure 22 shows the hydropower potential simulation using GCM1 across an across all time period. The figure provides a visual representation of the hydropower potential trend from the year 2030 to 2100. In this analysis, a prominent pattern emerges, characterized by both substantial increases and decreases in hydropower potential over this time period. Initiating from 2030, the hydropower potential commences at a maximum value of 410 MWh. This upward trajectory signifies a period of significant potential for energy generation. However, as time progresses towards 2100, the trend takes a notable turn. The hydropower potential experiences a decline, reaching a value of 170-250 MWh.

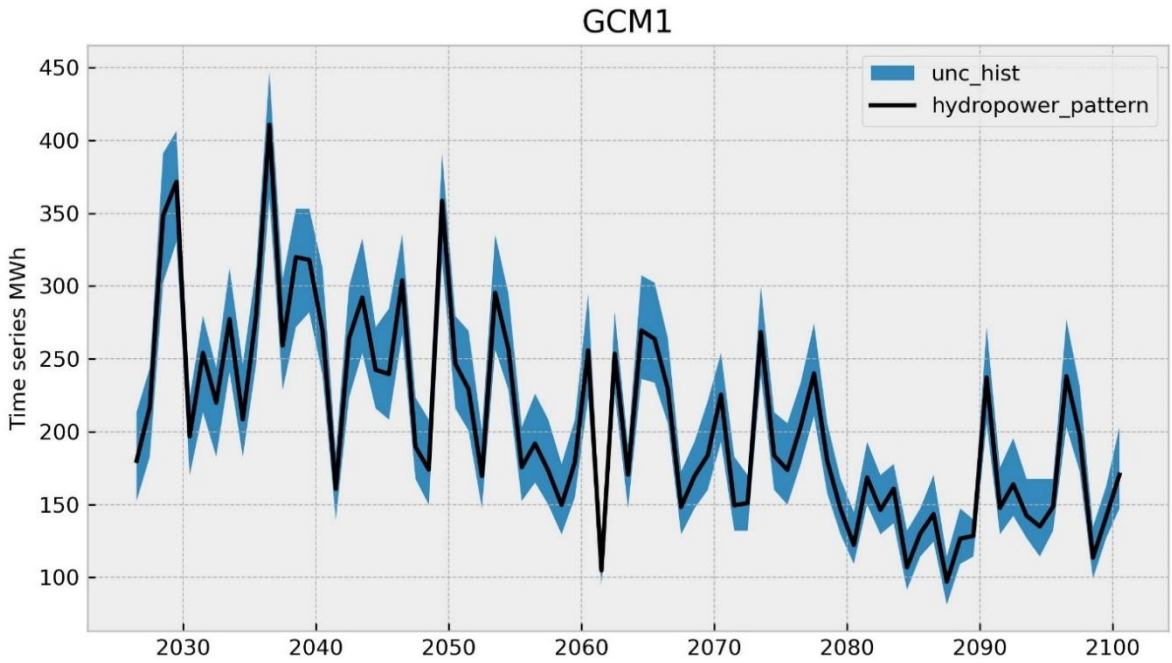

Figure 22 Time series plot of hydropower potential over the future period from 2025-2100 We calculate the time series of hydropower potential by assessing the potential energy that can be generated from water over a period.

Figure 23 show the time series of hydropower potential simulation using GCM2 across all time period. This figure offers a visual representation of the hydropower potential trend from the year 2030 to 2100. A distinct pattern is evident, characterized by noteworthy oscillations in hydropower potential over this extended time period. Beginning in 2030, For instance the hydropower potential starts at a significant value of 480 MWh. This initial surge indicates a promising period of robust energy generation potential. However, as the timeline progresses towards 2100, the trend experiences a significant shift. The hydropower potential takes a pronounced downturn, decreasing to a value of 110-200 MWh. This decline raises the possibility of altered hydrological dynamics or broader climatic influences impacting energy generation patterns.

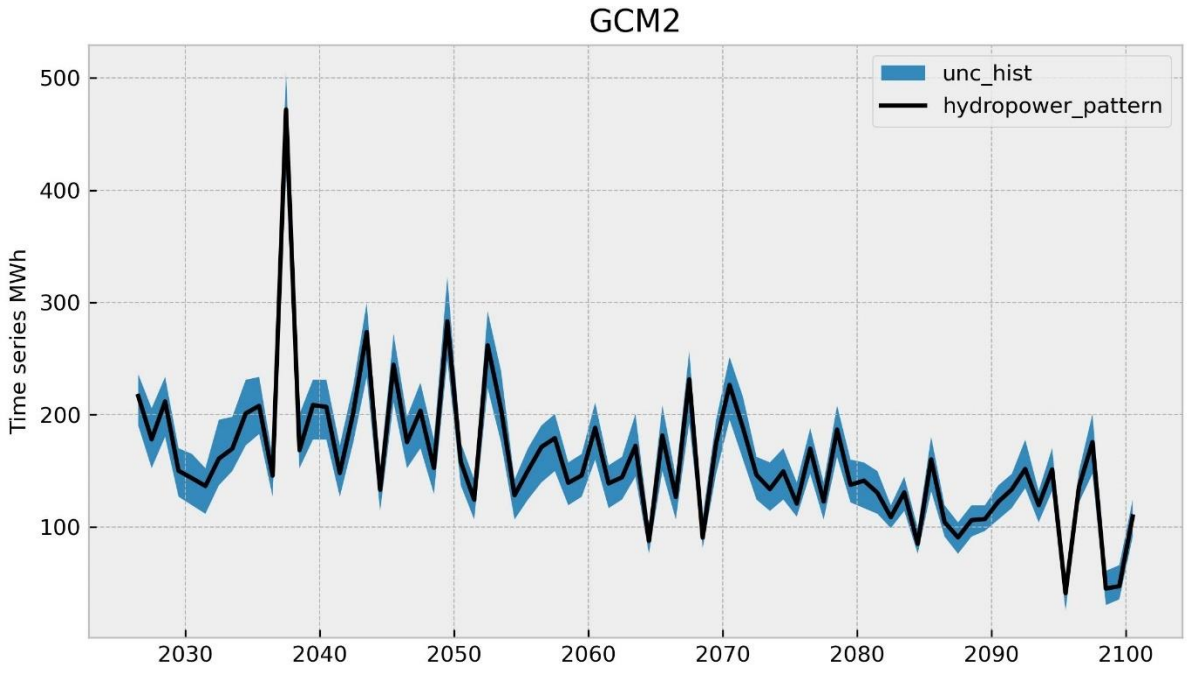

Figure 23: Time series plot of hydropower potential over the future period from 2025-2100 We calculate the time series of hydropower potential by assessing the potential energy that can be generated from water over a period.

Figure 24 shows the time series of hydropower potential simulation using GCM3across all time period. This visual representation displays the trend in hydropower potential from the year 2030 to 2100. A distinctive pattern emerges, characterized by substantial fluctuations in hydropower potential across this extended timeframe. For instance, in 2030, the hydropower potential initiates at a considerable level of 260 MWh. This initial surge signifies a period of promising energy generation potential. However, as the timeline progresses towards 2100, a notable shift

unfolds. The trend takes a distinct downturn, with the hydropower potential decreasing to a value of 150-200 MWh. This decline prompts consideration of evolving hydrological dynamics or broader climatic influences influencing energy generation patterns.

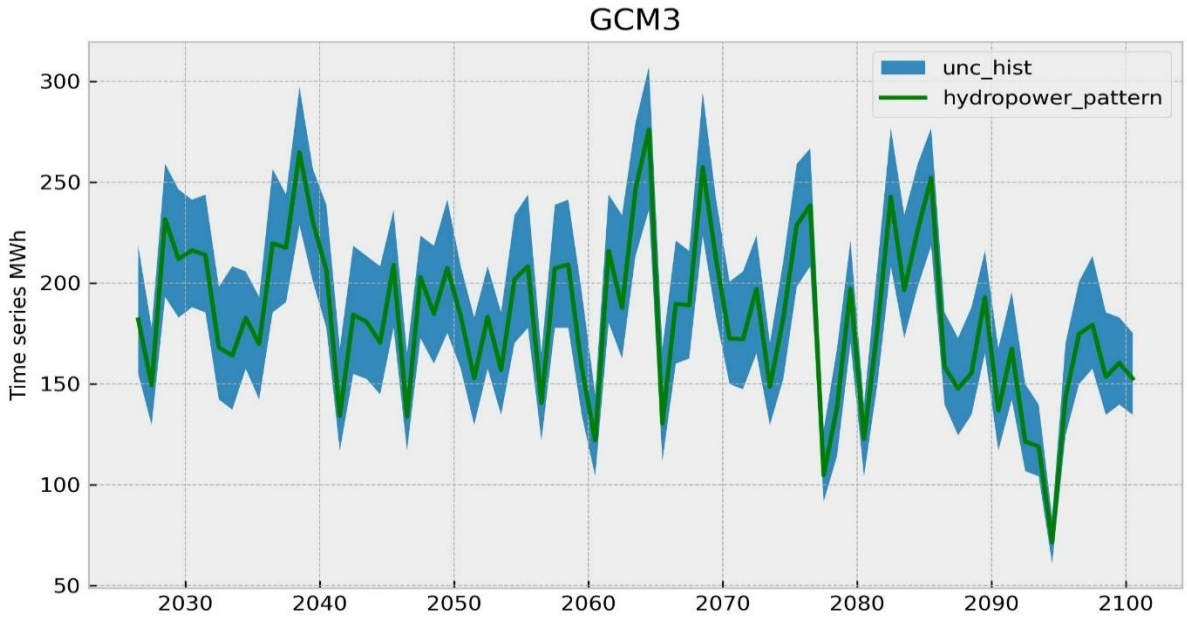

Figure 24: Time series plot of hydropower potential over the future period from 2025-2100 We calculate the time series of hydropower potential by assessing the potential energy that can be generated from water over a period of time.

The hydropower potential simulations presented in Figures 22, 23, and 24 provide valuable insights into the potential trends and variability of energy generation over an extended time period. The analysis highlights the complex interplay between climate dynamics and energy generation, with distinct patterns emerging across different GCMs and time periods.

The hydropower potential simulations presented in Figures 22, 23, and 24 provide valuable insights into the potential trends and variability of energy generation over an extended time period. The analysis highlights the complex interplay between climate dynamics and energy generation, with distinct patterns emerging across different GCMs and time periods.

Figure 22 illustrates the hydropower potential simulation using GCM1. The initial years, starting from 2030, exhibit a promising trend characterized by a substantial increase in hydropower potential, reaching a maximum value of 410 MWh. This signifies a period of considerable energy generation potential. However, the subsequent decades show a marked decline, with the hydropower potential decreasing to a range of 170-250 MWh by 2100. This downturn raises important questions about the drivers behind such a shift and the implications

for long-term energy planning and sustainability. In Figure 23, the hydropower potential simulation using GCM2 reveals a distinct pattern of oscillations in energy potential from 2030 to 2100. The initial surge in hydropower potential, reaching 480 MWh, suggests a period of robust energy generation prospects. However, the following years display a significant decline, with the potential dropping to 110-200 MWh. This trend prompts consideration of whether changing hydrological patterns or broader climatic influences play a role in shaping energy potential fluctuations. Figure 24 depicts the hydropower potential simulation using GCM3, revealing a fluctuating pattern across the time period. The initial years, starting with a hydropower potential of 260 MWh in 2030, indicate a promising outlook for energy generation. Nonetheless, as time progresses towards 2100, a distinct downturn is observed, with the potential decreasing to a range of 150-200 MWh. This decline raises important questions about the drivers of such changes and underscores the need to consider evolving hydrological dynamics and broader climatic factors. The trends observed in the hydropower potential simulations across the different GCMs and time periods have significant implications for energy planning and policy development. The initial periods of robust energy generation potential underscore the importance of harnessing hydropower resources for sustainable energy production. However, the subsequent declines in hydropower potential raise concerns about the long-term reliability of such energy sources and the need for diversification and adaptation strategies.

In conclusion, the analysis of hydropower potential simulations using different GCMs across time periods contributes to our understanding of the complex relationship between climate dynamics and energy generation. The observed trends highlight the importance of adaptive energy planning that considers potential fluctuations in hydropower resources due to changing hydrological and climatic conditions.

4.2 **Long-term average change in Hydropower Potential**

Figure 25 shows the long-term average change in hydropower potential across the historical period and three future periods. The data presented in the figure indicates a consistent trend of decreasing hydropower potential in the future periods when compared to the historical period. Across the three General Circulation Models (GCMs), the historical period demonstrates an average hydropower potential of ca 210 MWh. However, this value undergoes noticeable changes in the future periods. In the future period, the average potential increases to ca 170 MWh, followed by a decrease to 140 MWh in the far future period. These changes represent shifts of 19% and 33% respectively when compared to the historical period.

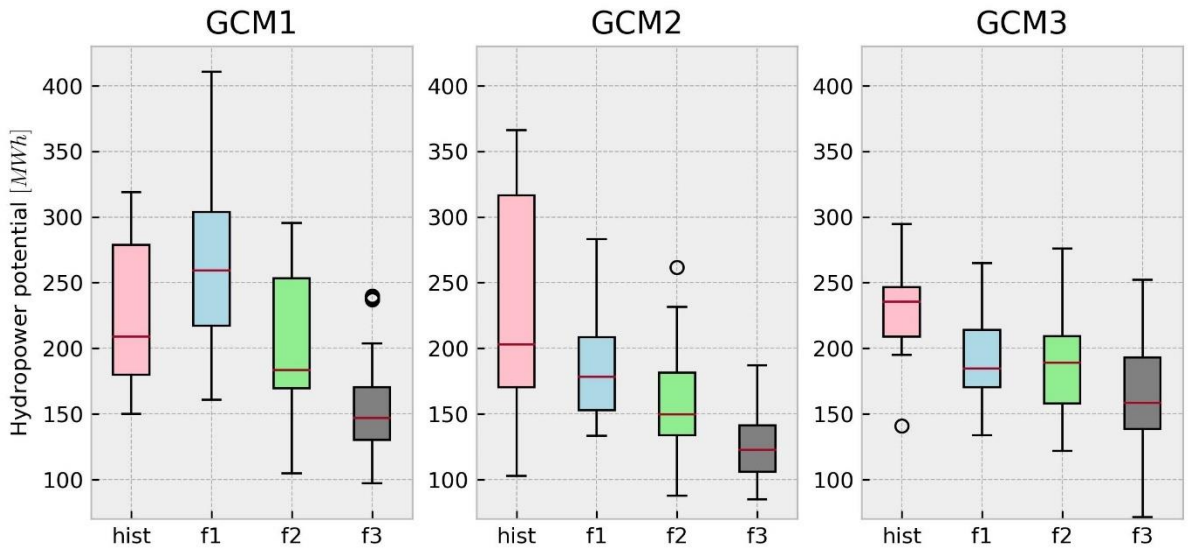

Figure 25 Change in hydropower potential for three (GCMs)-GCM1, GCM2, and GCM3 across the historical period (1996-2005) and the future periods (near future, future, and far future -2011-2100). we calculated long-term average change in hydropower by analyzing historical data related to the streamflow.

The analysis depicted in Figure 25 provides a clear overview of the long-term average change in hydropower potential across different time periods. The data presents a consistent and concerning trend of decreasing hydropower potential in the future periods when compared to the historical period. This trend holds across all three General Circulation Models (GCMs) considered in the study.

The historical period serves as a baseline, with an average hydropower potential of approximately 210 MWh. This historical context is crucial for understanding the changes observed in the future periods. The data reveals distinct shifts in hydropower potential values for the future periods. In the near future period, the average potential increases slightly to around 170 MWh before declining further to approximately 140 MWh in the far future period. The observed changes in hydropower potential carry significant implications for energy generation and planning. The analysis highlights that the hydropower potential decreases by 19% in the future period and by 33% in the far future period when compared to the historical baseline. These magnitudes of change underscore the substantial challenges that may arise in maintaining consistent and reliable hydropower generation over time. The declining trend in hydropower potential raises questions about the factors driving these changes. Climate change, alterations in precipitation patterns, and shifts in hydrological cycles are likely contributors to the observed decline. It's important to consider how these changes may impact the availability of water resources that drive hydropower generation and how they might interact with other

environmental and societal factors. The decreasing trend in hydropower potential has direct implications for energy security and planning. As hydropower has historically been a reliable and renewable energy source, the diminishing potential introduces uncertainties into long-term energy strategies. Energy planners and policymakers need to consider how this decline might affect energy supply, grid stability, and the achievement of renewable energy goals.

The analysis of long-term average change in hydropower potential presented in Figure 25 highlights the key findings of the study and the challenges posed by decreasing hydropower potential in the face of changing climatic conditions. The consistency of this trend across different GCMs underscores the urgency of addressing these challenges. This contributes valuable insights into the potential impacts of climate change on energy generation and underscores the importance of adaptive energy planning strategies for a sustainable and secure energy future.

4.3 Annual Change in Hydropower Potential

Figure 26 below shows the annual change trends in hydropower potential for GCM1 across different months. In comparing the historical period to the future periods, minimal variation is observed from January to April. However, a distinct pattern emerges from May to October, indicating an increase in hydropower potential. There's a gradual rise in hydropower potential from 10 MWh in May to 45 MWh in October for the near future period. This increase highlights the variability in hydropower generation potential during these months. The future periods continue to demonstrate a downward trajectory. In the near future, hydropower potential extends from 10 MWh to 55 MWh over the same months, with a maximum uncertainty of 60 MWh. The future period maintains a range of 10 MWh to 45 MWh, coupled with an uncertainty of 50 MWh. Similarly, the far future period displays hydropower potential fluctuating from 10 MWh to 40 MWh, accompanied by an uncertainty of 45 MWh.

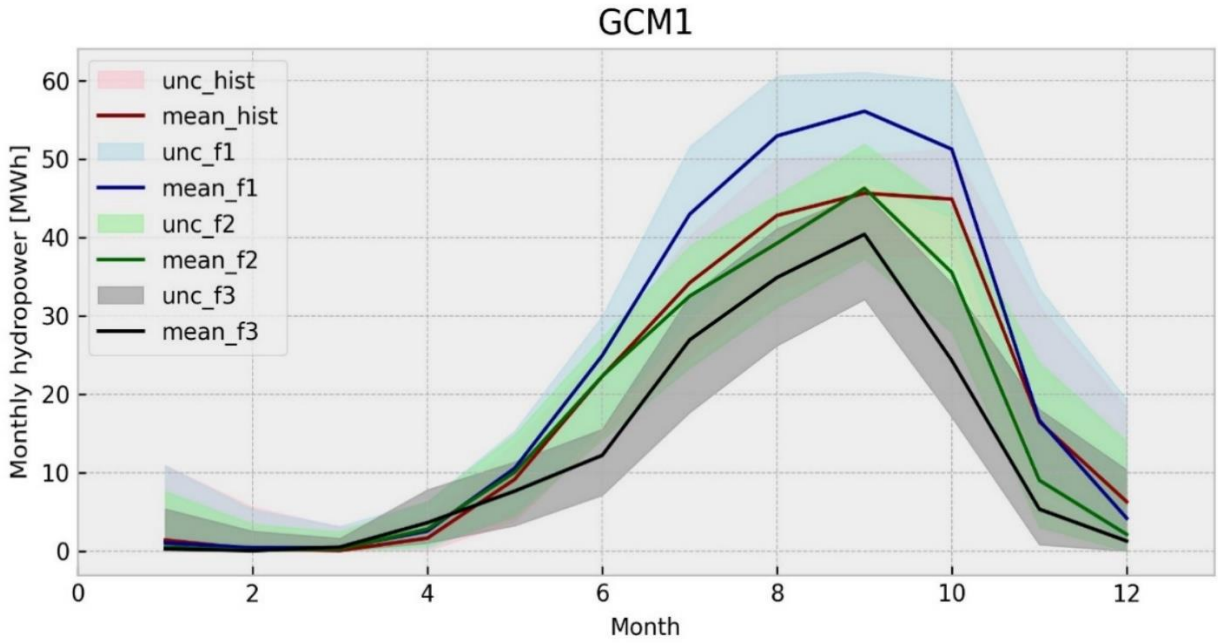

Figure 26 Monthly hydropower patterns of GCM1 for the historical period (1996-2005) and the three future periods (2011-2100). We calculated the annual change in hydropower potential by comparing the energy to the flow rate of one year

Figure 27 shows the annual change trends in hydropower potential for GMC2 across different months. In comparing the historical period to three future periods, there is minimal variation observed from January to March. However, from April to December, both historical and future periods exhibit fluctuating trends in hydropower potential. Notably, the maximum trend of hydropower potential is observed in April with a value of 43 MWh, accompanied by an uncertainty reaching to 58 MWh. As we transition to the future periods, the dynamics shift. The near future period portrays a decrease to 30 MWh in April, with an associated uncertainty of 35 MWh. Similarly, the future period experiences a further reduction to 25 MWh in April, along with an uncertainty of 28 MWh. Finally, the far future period shows the lowest value of 18 MWh in April, with an uncertainty of 20 MWh.

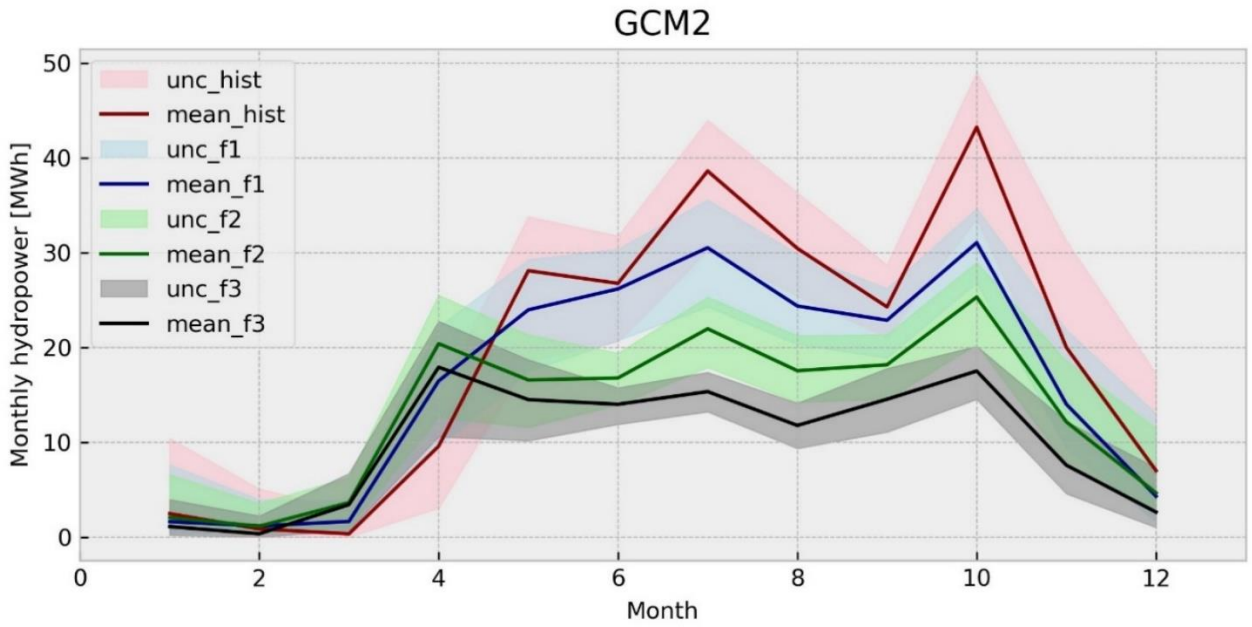

Figure 27 Monthly hydropower patterns of GCM2 for the historical period (1996-2005) and the three future periods (2011-2100). We calculated the annual change in hydropower potential by comparing the energy to the flow rate of one year.

Figure 28 shows the annual change trends in hydropower potential for GCM3 across different months. In comparing the historical period to the future periods, minimal variation is observed from January to March. However, a distinct pattern emerges from April to December, indicating an increase in hydropower potential. The future periods continue to demonstrate an downward trajectory. In the near future, hydropower potential extends from 10 MWh to 48 MWh over the same months, with a maximum uncertainty of 60 MWh. The future period maintains a range of 10 MWh to 53MWh, coupled with an uncertainty of 50 MWh. Similarly, the far future period displays hydropower potential fluctuating from 10 MWh to 43 MWh, accompanied by an uncertainty of 45 MWh.

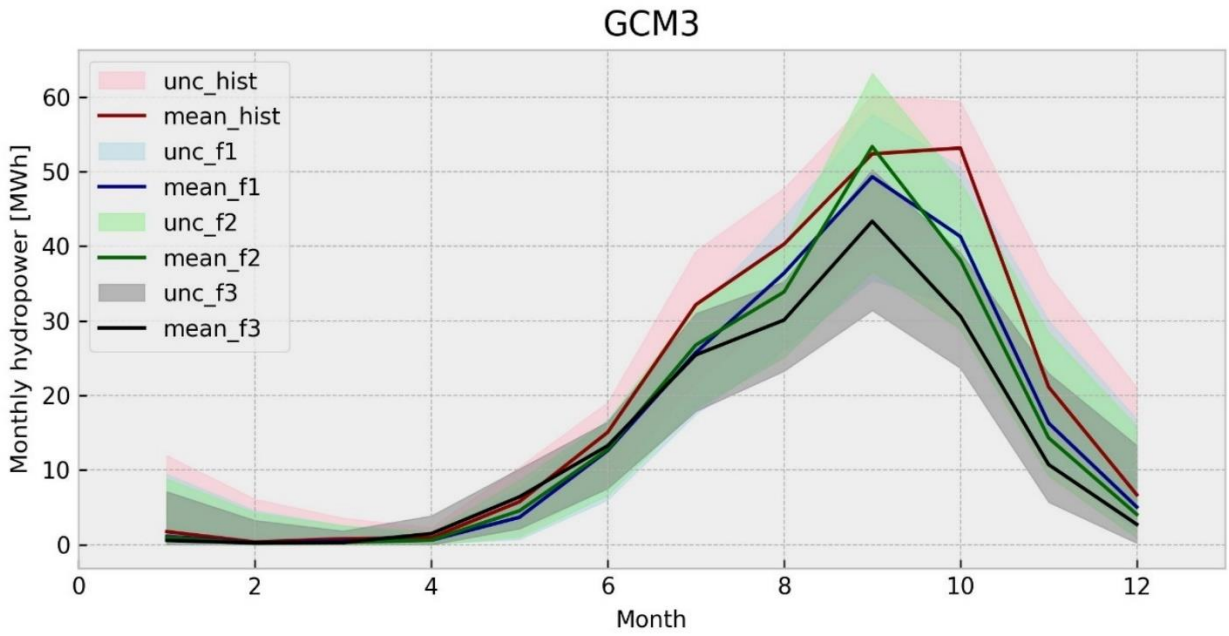

Figure 28 illustrates the monthly hydropower patterns of GCM3 for the historical period (1996-2005) and the three future periods (2011-2100). We calculated the annual change in hydropower potential by comparing the energy to the flow rate of one year

The analysis depicted in Figures 26, 27, and 28 offers valuable insights into the annual change trends in hydropower potential across different months for various General Circulation Models (GCMs) and time periods. These figures highlight the seasonality of hydropower generation potential and the variations that emerge as a result of changing climatic conditions.

In Figure 26, the annual change trends in hydropower potential using GCM1 reveal interesting patterns. Minimal variation is observed from January to April across the historical and future periods. However, from May to October, a distinct pattern of increasing hydropower potential emerges. The near future period displays a rise from 10 MWh in May to 55 MWh in October, showcasing the variability in hydropower generation potential during these months. The subsequent future periods show a downward trajectory, indicating the need for a careful assessment of the energy generation potential during these months. Figure 27 illustrates the annual change trends in hydropower potential using GCM2. While minimal variation is observed from January to March, significant changes occur from April to December for both historical and future periods. Notably, April exhibits the highest trend in hydropower potential at 43 MWh, with associated uncertainty. The transition to the future periods introduces fluctuations, with the near future period showing a decrease to 30 MWh in April. This shift underscores the dynamic nature of hydropower potential and its sensitivity to changing climatic

conditions. The analysis in Figure 28 presents the annual change trends in hydropower potential using GCM3. Similarly, to GCM1, minimal variation is observed from January to March. However, April to December showcases an increase in hydropower potential for both the future periods, deviating from the historical trend. The increasing trend in hydropower potential during these months emphasizes the need to consider potential shifts in water availability and hydrological cycles when planning for energy generation. The seasonal variation in hydropower potential observed in these figures underscores the complexities of energy planning in the context of changing climatic conditions. The fluctuations in potential from month to month and from historical to future periods necessitate a flexible and adaptive approach to energy resource management.

However, the Changes in potential hydropower generation in Africa may impact future hydropower generation in the region. These findings reveal that climate change is likely to have a significant impact of decrease in the average hydropower generation by 31% in future periods. This is due to rising temperatures and low runoff with potential implications on energy security and sustainability. These findings align with (Freitas & Soito, 2009), which reveal that global warming and changes in the water cycle can disrupt the availability and distribution of hydropower resources. Their analysis confirms the link between climate change and hydropower potential, as demonstrated by the varying patterns in hydropower generation across different periods and General climate models (GCMs). The time series plot depicts a range of values, indicating uncertainty in the future hydropower potential. These results from the three GCMs exhibit divergent trends, with GCM1 showing a slight decrease in hydropower potential, compared to GCM2 &GCM3 projecting a substantial decrease due to rising temperature and less precipitation. These differences underline the complexity and uncertainty in forecasting hydropower generation under changing climate conditions, as noted by (Fan et al., 2020). Contrary to Fan et al. (2020), X. Liu et al. (2016) indicated that hydropower potential can be attributed to climate-induced variations in rainfall and temperature. They stated that increased rainfall positively correlates with higher hydropower generation due to increased runoff and water storage in reservoirs promoting production. On the other hand, X. Liu et al. (2016) also contradict themselves indicating that rising temperature directly impacts hydropower generation by reducing reservoir storage capacity and limiting the overall generation potential.

This finding is consistent with emphasis the vulnerability of hydropower systems to the impacts of climate change (Abraham et al., 2022). Their analysis also highlights the importance of considering seasonality in a generation.

PARTICAL CONCLUSION

Chapter three presents an analysis on precipitation patterns, temperature, streamflow, and potential hydropower generation. The study reveals a significant decrease in long-term average precipitation from historical to far future periods. It also examines climate change impacts through temperature trends analysis, which shows an upward increase in temperatures across historical and future periods. The most significant increase is predicted by GCM1, rising from 21°C in the historical period to 26°C in the far future. GCM2 and GCM3 also predict significant increases, with average temperatures averaging 19.3°C in the historical period and 21.2°C, 22.23°C, and 24°C respectively in the near future, future, and far future periods. The anticipated decrease in streamflow is a major concern for water resource management strategies, particularly in the context of hydropower generation. To address these potential impacts, adaptation measures such as water conservation, efficient irrigation practices, and resilient water management plans are crucial. The data shows distinct shifts in hydropower potential values, with a 19% decrease in the near future period and 33% in the far future period relative to the historical baseline.

CONCLUSION AND PERSPECTIVES

CONCLUSION AND PERSPECTIVES

The finding from the study on the impact of changing climate on streamflow for potential hydropower Generation in Africa, Genale Dawa III Ethiopia have significant implications for the sustainable planning and management of hydropower dam in the catchment and potentially other regions in Africa. With climate change projections indicating uncertain and diverse outcome, policymakers, energy planning and stakeholders must adopt adaptive strategies and robust planning approaches. Climate change adaptation measures, such as reservoir management strategies, infrastructure upgrades and efficient water resource management, will be essential to ensure the long-term viability of hydropower projects in the face of changing climate condition in the future periods. The study also highlights the uncertainties associated with climate projections and emphasizes the importance of understanding potential changes in precipitation, temperature, streamflow, and hydropower potential in the Genale Dawa III(GD-3) catchment. In so doing governments and policymakers in Africa need to adopt proactive measures to address the impacts of changing climate on hydropower generation, and also the implementation of climate change mitigation strategies in addressing the challenges posed by changing streamflow patterns on hydropower generation in the future periods.

1. **Limitation of the study**

While the study provides valuable insights into establishing the relationship between streamflow and hydropower potential, The study analyze how climate change affects the annual hydropower electricity generation, and investigates the impact of climate change on the seasonal hydropower potential, The potential impact of climate change on streamflow and hydropower generation in the Genale Dawa III catchment. However, it is essential to acknowledge some limitations that may affect the interpretation and generalization of the results. Such limitations include Data Limitations, Climate Model Uncertainty, Sensitivity to Model Parameters, Hydropower Technology Assumptions, Assumptions of Emission Scenarios, and Long-Term Projections Uncertainty for streamflow and the hydropower generation. Future research can address this limitation to further enhance the understanding of the potential impacts of climate change on streamflow and hydropower generation in the Genale Dawa III catchment by improving model accuracy, and exploring ensemble approaches to provide a clearer understanding of potential future streamflow patterns.

2. Outlook of this research

The outlook of this study on the impact of changing climate on streamflow for potential hydropower generation in Africa can incorporate the Investigation of evapotranspiration rates in the study area to determine the reasons for decrease in the hydropower potential and uncertainty. The outlook could also include climate change adaptation, ecological impact, and water-energy nexus.

BIBLOGRAPHY REFERENCES

Beck, H. E., Pan, M., Lin, P., Seibert, J., Dijk, A. I. J. M., & Wood, E. F. (2020). Global Fully Distributed Parameter Regionalization Based on Observed Streamflow From 4,229 Headwater Catchments.*JournalofGeophysicalResearch:Atmospheres*,*125*(17).https://doi.org/10.1029/2019JD031485

Beheshti, M., Heidari, A., & Saghafian, B. (2019). Susceptibility of Hydropower Generation to Climate Change: Karun III Dam Case Study. *Water*, *11*(5), 1025. https://doi.org/10.3390/w11051025

Bergström, S. (1976a). DEVELOPMENT AND APPLICATION CONCEPTUAL RUNOFF MODEL FOR SCANDINAVIAN CATCHMENTS.

Bergström, S. (1976b). DEVELOPMENT AND APPLICATION CONCEPTUAL RUNOFF MODEL FOR SCANDINAVIAN CATCHMENTS.

Bergström, S., & Forsman, A. (1973). DEVELOPMENT OF A CONCEPTUAL DETERMINISTIC RAINFALL-RUNOFF MODEL. *Hydrology Research*, *4*(3), 147–170. https://doi.org/10.2166/nh.1973.0012

Cáceres, A. L., Jaramillo, P., Matthews, H. S., Samaras, C., & Nijssen, B. (2022). Potential hydropower contribution to mitigate climate risk and build resilience in Africa. *Nature Climate Change*, *12*(8), 719–727. https://doi.org/10.1038/s41558-022-01413-6

Chen, Y.-J., Chu, J.-L., Tung, C.-P., & Yeh, K. C. (2016). Climate Change Impacts on Streamflow in Taiwan Catchments Based on Statistical Downscaling Data.*Terrestrial, Atmospheric andOceanicSciences*,*27*(5),741–755. https://doi.org/10.3319/TAO.2016.07.20.01

De Oliveira, V. A., De Mello, C. R., Viola, M. R., & Srinivasan, R. (2017). Assessment of climate change impacts on streamflow and hydropower potential in the headwater region of the Grande river basin, Southeastern Brazil: CLIMATE CHANGE IMPACTS ON

STREAMFLOW AND HYDROPOWER POTENTIAL. *International Journal of Climatology*, *37*(15), 5005–5023. https://doi.org/10.1002/joc.5138

Devia, G. K., Ganasri, B. P., & Dwarakish, G. S. (2015). A Review on Hydrological Models. *Aquatic Procedia*, *4*, 1001–1007. https://doi.org/10.1016/j.aqpro.2015.02.126

Fan, J.-L., Hu, J.-W., Zhang, X., Kong, L.-S., Li, F., & Mi, Z. (2020). Impacts of climate change on hydropower generation in China. *Mathematics and Computers in Simulation*, *167*, 4–18. https://doi.org/10.1016/j.matcom.2018.01.002

Freitas, M. A. V., & Soito, J. L. S. (2009). *Vulnerability to climate change and water management: Hydropower generation in Brazil*. 217–226. https://doi.org/10.2495/RM090201

Hamududu, B., & Killingtveit, A. (2012). Assessing Climate Change Impacts on Global Hydropower. *Energies*, *5*(2), 305–322. https://doi.org/10.3390/en5020305

Kankam-Yeboah, K., Obuobie, E., Amisigo, B., & Opoku-Ankomah, Y. (2013). Impact of climate change on streamflow in selected river basins in Ghana. *Hydrological Sciences Journal*, *58*(4), 773–788. https://doi.org/10.1080/02626667.2013.782101

Larbi, I., Nyamekye, C., Dotse, S.-Q., Danso, D. K., Annor, T., Bessah, E., Limantol, A. M., Attah-Darkwa, T., Kwawuvi, D., & Yomo, M. (2022). Rainfall and temperature projections and the implications on streamflow and evapotranspiration in the near future at the Tano River Basin of Ghana. *Scientific African*, *15*, e01071. https://doi.org/10.1016/j.sciaf.2021.e01071

Liu, N., Harper, R. J., Smettem, K. R. J., Dell, B., & Liu, S. (2019). Responses of streamflow to vegetation and climate change in southwestern Australia. *Journal of Hydrology*, *572*, 761–770. https://doi.org/10.1016/j.jhydrol.2019.03.005

Liu, X., Tang, Q., Voisin, N., & Cui, H. (2016). Projected impacts of climate change on hydropower potential in China. *Hydrology and Earth System Sciences*, *20*(8), 3343–3359. https://doi.org/10.5194/hess-20-3343-2016

Nonki, R. M., Lenouo, A., Tchawoua, C., Lennard, C. J., & Amoussou, E. (2021). Impact of climate change on hydropower potential of the Lagdo dam, Benue River Basin, Northern Cameroon. *Proceedings of the International Association of Hydrological Sciences*, *384*, 337–342. https://doi.org/10.5194/piahs-384-337-2021

Seibert, J. (1999). Regionalisation of parameters for a conceptual rainfall-runoff model. *Agricultural and Forest Meteorology*, *98–99*, 279–293. https://doi.org/10.1016/S0168-1923(99)00105-7

Seibert, J., & Vis, M. J. P. (2012). Teaching hydrological modeling with a user-friendly catchment-runoff-model software package. *Hydrology and Earth System Sciences*, *16*(9), 3315–3325. https://doi.org/10.5194/hess-16-3315-2012

Shigute, M., Alamirew, T., Abebe, A., Ndehedehe, C. E., & Kassahun, H. T. (2022). Understanding Hydrological Processes under Land Use Land Cover Change in the Upper Genale River Basin, Ethiopia. *Water*, *14*(23), 3881. https://doi.org/10.3390/w14233881

Sirisena, T. A. J. G., Maskey, S., Bamunawala, J., & Ranasinghe, R. (2021). Climate Change and Reservoir Impacts on 21st-Century Streamflow and Fluvial Sediment Loads in the Irrawaddy River, Myanmar. *Frontiers in Earth Science*, *9*, 644527. https://doi.org/10.3389/feart.2021.644527

Wan, W., Wang, H., & Zhao, J. (2020). Hydraulic Potential Energy Model for Hydropower Operation in Mixed Reservoir Systems. *Water Resources Research*, *56*(4). https://doi.org/10.1029/2019WR026062

Wan, W., Zhao, J., Popat, E., Herbert, C., & Döll, P. (2021). Analyzing the Impact of Streamflow Drought on Hydroelectricity Production: A Global-Scale Study. *Water Resources Research*, *57*(4). https://doi.org/10.1029/2020WR028087

Xu, C.-Y., & Singh, V. P. (2005). Evaluation of three complementary relationship evapotranspiration models by water balance approach to estimate actual regional evapotranspiration in different climatic regions. *Journal of Hydrology*, *308*(1–4), 105–121. https://doi.org/10.1016/j.jhydrol.2004.10.024

Zheng, H., Zhang, L., Zhu, R., Liu, C., Sato, Y., & Fukushima, Y. (2009). Responses of streamflow to climate and land surface change in the headwaters of the Yellow River Basin: RESPONSES OF STREAMFLOW TO CLIMATE. *Water Resources Research*, *45*(7). https://doi.org/10.1029/2007WR006665